Recruitment of apolipoprotein E facilitates Herpes simplex virus 1 release

Lifeng Liu[a,b#], Konrad Thorsteinsson[a,b], Sanduni Wasana Jayaweera[a], Damien Avinens[a], Fouzia Bano[a,b] Dario Conca [a,b], Hugo Lövheim[b,c], Anders Olofsson[a], Marta Bally[a,b#]

[a]Department of Clinical Microbiology, Umeå University, Sweden.

[b]Wallenberg Centre for Molecular Medicine, Umeå University, Sweden.

[c]Department of Community Medicine and Rehabilitation, Umeå University, Sweden.

[#]Correspondence

Lifeng Liu, lifeng.liu@umu.se; Marta Bally, marta.bally@umu.se. Department of Clinical Microbiology, Umeå University, Sweden.

Abstract

Over two decades, epidemiological studies have revealed that interactions between human polymorphic apolipoprotein 4 (ApoE, isoform 4) and herpes simplex virus type 1 (HSV1) associate with higher risk of Alzheimer's disease, a serious and increasing issue among elder populations worldwide. Nevertheless, little is known about the mechanisms behind ApoE-HSV1 interactions at molecular levels. Here, we investigate the effects of ApoE on the HSV1 infectious life cycle in in vitro cell experiments. Analysis of HSV1 growth curves shows that HSV1 production is promoted in presence of any of the three ApoE isoforms, with ApoE 3or 4 demonstrating more efficient pro-viral effects than ApoE 2. When added prior to infection, ApoE inhibits viral attachment but does not affect viral entry. qPCR-based quantification reveals that harbouring ApoE 2, 3, or 4 leads to an increase of HSV1 extracellular release but unchanged levels of viral genome copies within cells or on the cell surface, indicating that virus replication, assembly, or transport to cell membrane are not affected. Further test of virus release directly demonstrates that HSV1 detachment from the cell surface is promoted by ApoE. Subsequent results reveal that ApoE is not only present in purified HSV1 particles produced in ApoE-expressing cells after ultra-centrifugation but also able to incorporate into HSV1 particles after purification, suggesting that harbouring ApoE may promote HSV1 detachment. With the help of total internal reflection microscopy (TIRFM), this hypothesis was tested by quantifying interaction kinetics and apparent affinity between of HSV1 and native supported lipid bilayer. HSV1 particle decorated with ApoE demonstrates higher dissociation rate constants (k_{off}) and less irreversible binding to the membrane, which is in line with the promoted virus release. Similar interaction kinetics have also been tested between non-decorated HSV1 particles and membranes harbouring ApoE but revealed no difference in the kinetics of virus particles on membranes with ApoE present or absent. Overall, our results provide new insights into the roles of ApoE during HSV1 infections, which is worth to be considered when studying their involvement during AD development.

Introduction

A possible involvement of herpes simplex virus 1 (HSV1) in the development of Alzheimer's disease (AD) a neurodegenerative disease with increasing threats among elder populations, was first suggested in the 80s (Ball, 1982); in the later years, epidemiological studies have strengthened this hypothesis. One key finding of population-based cohort studies is the likely interaction effect of HSV-1 and the apolipoprotein E allele 4 (E4) *APOE4* on AD, where these factors together associate with an increased risk of developing AD (R. F. Itzhaki et al., 2001; Ruth F. Itzhaki et al., 1997; Lin et al., 1996; Linard et al., 2020; K Lopatko Lindman et al., 2019; Lövheim et al., 2019; Steel & Eslick, 2015; Strandberg et al., 2005). Given that *APOE4* is such an established and strong AD risk factor, this interaction in turns provides strong support for a role of HSV-1 infection in AD processes. Along these lines, a few studies have also linked *APOE* genotype to cold sore frequency or anti-HSV IgM antibody presence, indicative of an effect on the immunological control over HSV1(LIN et al., 1995; Karin Lopatko Lindman et al., 2022; Pandey et al., 2020). Still, considering the potential importance of the interaction between *APOE* genotype and HSV-1 for AD risk, surprisingly little is known about how human apolipoprotein E (ApoE) and HSV1 interact mechanistically during virus infection.

Human apolipoprotein E (ApoE) is a polymorphic and multi-functional protein, 299 amino acids in length and containing two structural domains identified as the N-terminal (amino acids 1 – 191) and C-terminal domains (amino acids ~ 206 – 299), connected by a linker. Functional regions located in the two domains include the receptor binding and heparan sulphate binding regions in the N-terminal domain, as well as the lipid binding and self-association regions in the C-terminal domain (reviewed in (Tudorache et al., 2017)). The *ApoE* gene is located on human chromatin 19 (Myklebost & Rogne, 1988) and produces three major alleles, that encode three corresponding protein products termed ApoE 2, ApoE 3, and ApoE 4. These three ApoE isoforms differ at only two amino acid residues: 112 and 158; ApoE 3 has a cysteine at residue 112 and an arginine at 158; while at both sites ApoE 2 has cysteines and ApoE 4 has arginines. These single amino acid substitutions lead to important changes in the ApoE structure which in turn results in differences in the characteristics of the protein's receptor, as well as lipid and heparan sulphate binding abilities (reviewed in (Mahley & Rall Jr., 2000)). For example, ApoE 2 shows significantly lower binding affinity than ApoE 3 or 4 to the low density lipoprotein (LDL) receptor on cultured cells, which is thought to be a result of the missing arginine at 158 (Dong et al., 1996). The arginine 112 in ApoE 4 enables unique domain interactions, accounting for its preference to very low density lipoproteins (VLDL), in comparison to binding to high density lipoprotein by ApoE 2 or ApoE 3 (Dong & Weisgraber, 1996). In addition, a biomolecular interaction study using surface plasmon resonance has observed that ApoE 4 shows significant higher binding than ApoE 3 or ApoE 2 to the glycosaminoglycans (GAG) heparan sulphate and dermatan sulphate found on the cell surface, which is postulated to be a result of electrostatic interactions with the N-terminal domain (Yamauchi et al., 2008). The role of ApoE in biological processes has been investigated beyond its conventional

function in cholesterol transport; the protein has been shown to play roles in immune regulation, in virus infection and in the development of cardiovascular and neurological diseases (summarized in (Tudorache et al., 2017)). For decades, carrying the allele *ApoE4* has been seen as the most important risk factor for the development of sporadic Alzheimer's disease, (see review (Kim et al., 2009)). Nevertheless, mechanistic insights on why ApoE 4 increases AD susceptibility are widely lacking, and the protein alone is not a strong risk factor for AD development, suggesting the involvement of other factors, such as an infection history with some human neurotropic pathogens. Many studies have suggested that herpesvirus infection, and in particular infection with HSV1, could be one of the important pathogenic factors for the AD development (Wainberg et al., 2021).

HSV is a human neurotropic virus member of the alpha Herpesviridae subfamily, which exists as two major serotypes HSV1 and HSV2. The prevalence of infection is estimated to be as high as 67% for HSV1 and 13% for HSV2 among people under age 50 ("Herpes simplex virus". World Health Organization. 31 January 2017). One of the biological features of HSV infection is that the virus can produce lytic or latent infections, depending on the target cell types. HSV1 establishes a lifelong latency in neurons specifically but undergoes lytic cycles in other cell types after reactivation (Brown, 2017). The HSV virion is composed of three structural parts: an icosahedral capsid enclosing a linear, double-stranded DNA viral genome; a layer of proteins called tegument surrounding the capsid shell, and a glycoprotein-containing lipid membrane envelope as the outermost layer, wrapping both the tegument and nucleocapsid. The HSV DNA genome, approximately 152 kilo base pairs in length, encodes about 80 viral proteins, among which at least 12 of them are glycoproteins displayed on the envelope. Consistent with the large variety of glycoproteins found in the virion, HSV1 entry is a complex and versatile process which depends on the infected tissue and on the infection circumstances. Prior to entry, virus attachment is mediated by the interactions between virus glycoprotein B and C and GAGs on the cell surface, heparan sulphate (Shieh et al., 1992) or chondroitin sulfate proteoglycans (Banfield et al., 1995). Recent studies have characterized interactions between HSV glycoprotein B or C and various GAGs (Altgärde et al., 2015; Delguste et al., 2019; Peerboom et al., 2017; E Trybala et al., 2000) and revealed the interactions are important not only for virus attachment, but also for virus particle transport to entry receptors on cell surface (Abidine et al., 2022). These studies also highlight that the characteristics of such interactions need to be tightly regulated, not only to ensure efficient virus recruitment during entry but also efficient virus release upon egress. Glycoprotein o-glycosylation (Altgärde et al., 2015; Edward Trybala et al., 2021) but also increased heparinase expression upon infection (S. Hadigal et al., 2020; Hopkins et al., 2018b) have been proposed as important factors contributing to a balanced GAG-virus interaction at the cell surface.

Recent studies have revealed that ApoE plays important roles during infections with different viruses (Tudorache et al., 2017) and is involved in the corresponding pathogenesis and diseases (Kuhlmann et al., 2010). ApoE expression is upregulated in HIV-infected macrophages but inhibits HIV infection

when overexpressed in the 293T cell line (Siddiqui et al., 2018). In contrast, hepatotropic virus hepatitis B (HBV) and hepatitis C (HCV) viruses require ApoE for efficient infection and virus production, and ApoE has also been co-purified together with HBV and HCV particles, suggesting incorporation of the protein into virus particles (Bankwitz et al., 2017; Chang et al., 2007; Jiang & Luo, 2009; Qiao & Luo, 2019). Mechanistic studies suggest that virus attachment to HSPG on the cell surface is facilitated by ApoE for both HBV and HCV (Jiang et al., 2013; Li & Luo, 2021) and that virus assembly or egress of HCV also benefits from ApoE (Benga et al., 2010; Cun et al., 2010; Lee et al., 2014). However, none of these effects are isoform dependent. Isoform-dependent effects have been observed in some HSV1 studies. Transgenic mice studies show that in comparison to ApoE 3, ApoE 4 leads to more brain access (Burgos et al., 2006) and latency to HSV1 (P S Bhattacharjee et al., 2006; Miller & Federoff, 2008), as well as to more severe pathogenesis (P S Bhattacharjee et al., 2008). Moreover, ApoE derived peptides were found to inhibit HSV1 infection (Partha S. Bhattacharjee et al., 2008; Partha S Bhattacharjee et al., 2009; Dobson et al., 2006), likely by targeting HSPGs, a shared cell-surface receptor for both ApoE and HSV1 (Saito et al., 2003; Shieh et al., 1992). On the other hand, pro-viral effects of ApoE have been suggested in ApoE knockout mice, where HSV1 infection and transmission is decreased in different organs, such as spinal cord and brain (Burgos et al., 2002). In spite of pathogenesis studies in animal models, and although similar studies have been done with other viruses, such as HIV, HBV, or HCV, little is known about ApoE effects on HSV1 growth at molecular levels. Here we investigate HSV1 infection on cultured cell lines in the presence of different ApoE isoforms. Our results reveal dual roles of ApoE on HSV1 infection which both likely target processes occurring at the cell surface: the protein inhibits virus attachment but promotes virus release. Overall, HSV1 growth is promoted by ApoE, suggesting a dominant role in the context of promoting virus release.

Results

HSV1 growth is promoted by the presence of ApoE.

To study how the presence of ApoE affects HSV1 infection and explore potential differences between the allelic isoforms of the protein, we tested HSV1 growth in the presence of various concentrations of ApoE in both the neuronal blastoma cell line SH-SY5Y and an epithelial cell line commonly used for HSV1 studies, green monkey kidney cells (GMK). In both SH-SY5Y and GMK cells, ApoE expression levels were negligible as verified by western blot (Fig. S1a). This is in line with the notion that ApoE is mainly secreted by the liver or by astrocytes in the brain (Elshourbagy et al., 1985). HSV1 growth was thus investigated by adding ectopically expressed and purified ApoE solutions. In such experiments, solutions of isoform 2, 3 or 4 with designated concentrations were prepared in cell culture mediums and then added to cells after 1h inoculation of HSV1 at MOI 0.1. At 24 hpi, viruses released in the medium were harvested and titrated by plaque assays. The results show that HSV1 growth was increased with

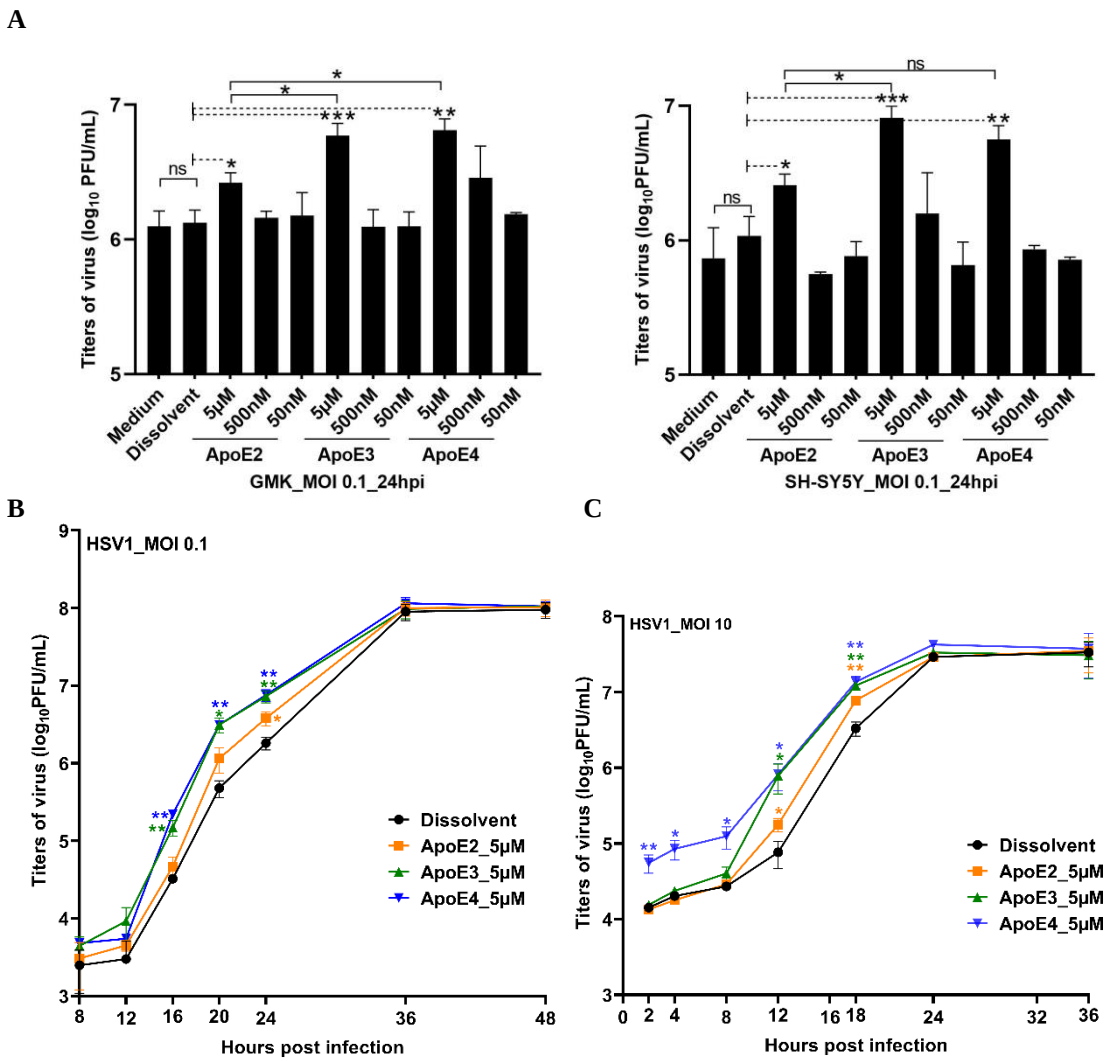

Fig. 1 HSV1 growth is accelerated by ApoE. (A) HSV1 growth was analysed by plaque assay at various concentrations of different ApoE isoforms on either GMK (left) or SH-SY5Y (right). **(B and C)** HSV1 growth kinetics of multiple **(B)** or single **(C)** infection cycles were studied on GMK with 5 µM of the different ApoE isoforms. Student t-test, ns=not significant, *: p≤0.05, **: p≤0.01, and ***: p≤0.001.

5 µM ApoE 3 or 5 µM ApoE 4 both on SH-SY5Y and GMK, but not by ApoE 2 or at lower concentrations of any of the apoE isoforms (Fig. 1A). There was no effect of the dissolvent on HSV1 growth as compared to that of the medium group, confirming that the increase of virus amounts in the supernatant resulted from the presence of ApoE. HSV1 growth was also tested on cells where apoE was added prior to, and kept during, the period of virus infection. Promotion of HSV1 growth was observed only with 5 µM ApoE 3 or 5 µM ApoE 4 to a similar extent as that in Fig. 1A, but not under other conditions (Fig. S1b), suggesting that apoE addition prior to infection was not additionally beneficial or detrimental under the investigated experimental conditions. Cell viability was tested in the presence of 5 µM ApoE 2, 3 or 4 confirming that none of the ApoE isoforms affected cell growth (Fig. S1c and

S1d). Considering that the phenotype is the same on both SH-SY5Y and GMK, and that GMK is commonly used for HSV1 research in the lab, which gives practical benefits to our study, we decided to work on GMK for the rest of our experiments.

Next, we investigated the HSV1 growth kinetics of multiple (MOI 0.1) or single infection (MOI 10) cycles on GMK in the presence of 5 µM ApoE isoforms. During multiple infection cycles (Fig. 1B), HSV1 in all groups had similar titers at shorter time points (< 12 hpi) and reached the same plateau values. However, in comparison to the dissolvent group, higher virus titers were detected at middle time points (16, 20 and 24 hpi) when ApoE was present (Fig. 1B). Such promotional effects are also isoform dependent, as more viruses were seen with ApoE 3 or 4 than with ApoE 2 at these timepoints (Fig. 1B). Similar as in multiple infection cycles, isoform dependent higher virus titers were also seen at middle timepoints (12 and 18 hpi) for ApoE groups as compared to the dissolvent group during virus single infection cycle, with more viruses detected in ApoE 3 or 4 group than ApoE 2 (Fig. 1C). An interesting observation was that for the ApoE 4 case under single infection cycle conditions (high MOI) more HSV1 viruses were detected at early time points, which most likely resulted from the release of viruses on the cell surface that had not been taken up, instead of promoted virus growth, in view of the short time after infection initiation. Considering the similar infection starts and plateaus, these results suggest that one or multiple steps of the HSV1 life cycle are promoted by ApoE, where ApoE 3 or 4 shows stronger effects than ApoE 2. Given that most HSV1 can successfully enter cells within the 1h inoculation (Nicola & Straus, 2004), the binding and entry in the first round of infection were unlikely studied with the experiment design where purified ApoE was added after the 1h inoculation. Nevertheless, ApoE was kept over the whole HSV1 infection cycles during multiple virus growth cycles, thus could be possibly involved in any infection stage during the following virus growth cycles. This made us investigate the potential roles of ApoE at different infection steps individually.

ApoE inhibits HSV1 attachment but does not affect virus entry efficiency.

Virus binding or entry was compared on GMK cells in the presence or absence of different ApoE isoforms. To compare virus binding, cells were treated with ApoE for 4 h prior to adding virus, followed by 1 h binding synchronization on ice with same amounts of virus in terms of PFUs. The attached viruses were quantified by qPCR. The results show that the presence of any of the three ApoE isoforms significantly reduced the amounts of HSV1 attached to cells, with the inhibitory effects being the strongest for ApoE 4 (Fig. 2A). The entry kinetics of HSV1 were analysed separately via a low-pH inactivation-based method on GMK cells mock treated or pre-treated with different ApoE. In brief, virus binding was synchronized for 1h with same PFUs (200 PFUs/well), as described above. Virus entry was then facilitated by increasing the temperature to 37°C for a selected period of time. At the selected time point, the remaining extracellular virus particles were inactivated by a low-PH buffer,

followed by agarose overlay for plaque formation and quantification. Time 0 where inactivation was done on ice before the temperature increase, was included as a control. At all the selected time points, including at 90 min when virus entry reached a plateau, we observed lower numbers of plaques in ApoE-treated groups as compared to the dissolvent group (Fig. 2B). The percentages of successfully entered viruses at 90 min reflected their binding propensity determined in the binding experiment (Fig. 2A), indicating that impaired virus entry is a result of reduced binding. This is further visualized in Fig. 2C displaying the entry efficiency over time, confirming that HSV1 entered cells at similar paces in all groups (Fig. 2C). These results reveal that HSV1 binding is hindered by the presence of ApoE, while entry is not affected.

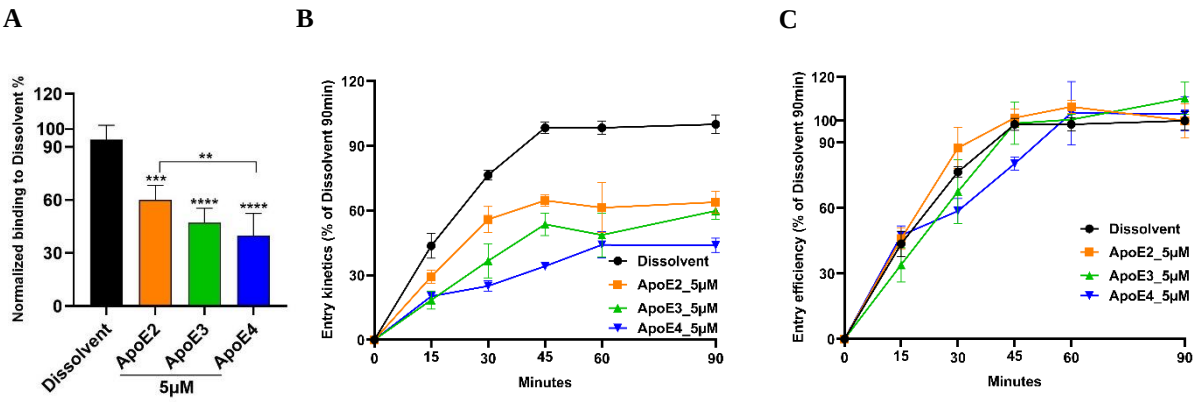

Fig. 2 HSV1 binding, but not entry, is affected by ApoE. (A) HSV1 attached to GMK cells, pre-treated with ApoE or dissolvent, were quantified by qPCR after 1 h binding synchronization on ice. The data of ApoE groups were normalized to the dissolvent group. **(B)** HSV1 entry to GMK treated with ApoE or dissolvent at selected timepoints were quantified by plaque formation. The average value of the dissolvent at 90 min was seen as the plateau, to which the rest of the data were normalized. **(C)** HSV1 entry efficiencies under different conditions were calculated by dividing the number of plaques by the binding ratios as shown in (A), followed by normalization as done for (B). Student t-test, ns=not significant, *: $p \leq 0.05$, **: $p \leq 0.01$, and ***: $p \leq 0.001$.

ApoE does not affect HSV1 replication or virus transport to the cell surface.

After binding and entry analysis, HSV1 replication was analysed by qPCR for genome quantification. At 24 hpi with HSV1 infection of MOI 0.1, supernatant and cell-associated viruses were harvested separately and quantified by plaque assays and qPCR respectively. Titration of the supernatant by plaque assays was included as a control and the results revealed increased viral titres in ApoE added groups (Fig. 3A, left Y axis), in agreement with previous data. In contrast, virus genome copies quantified by qPCR were similar in all groups (Fig. 3A, right Y axis). These results strongly suggest that ApoE promotes HSV1 release without affecting its replication.

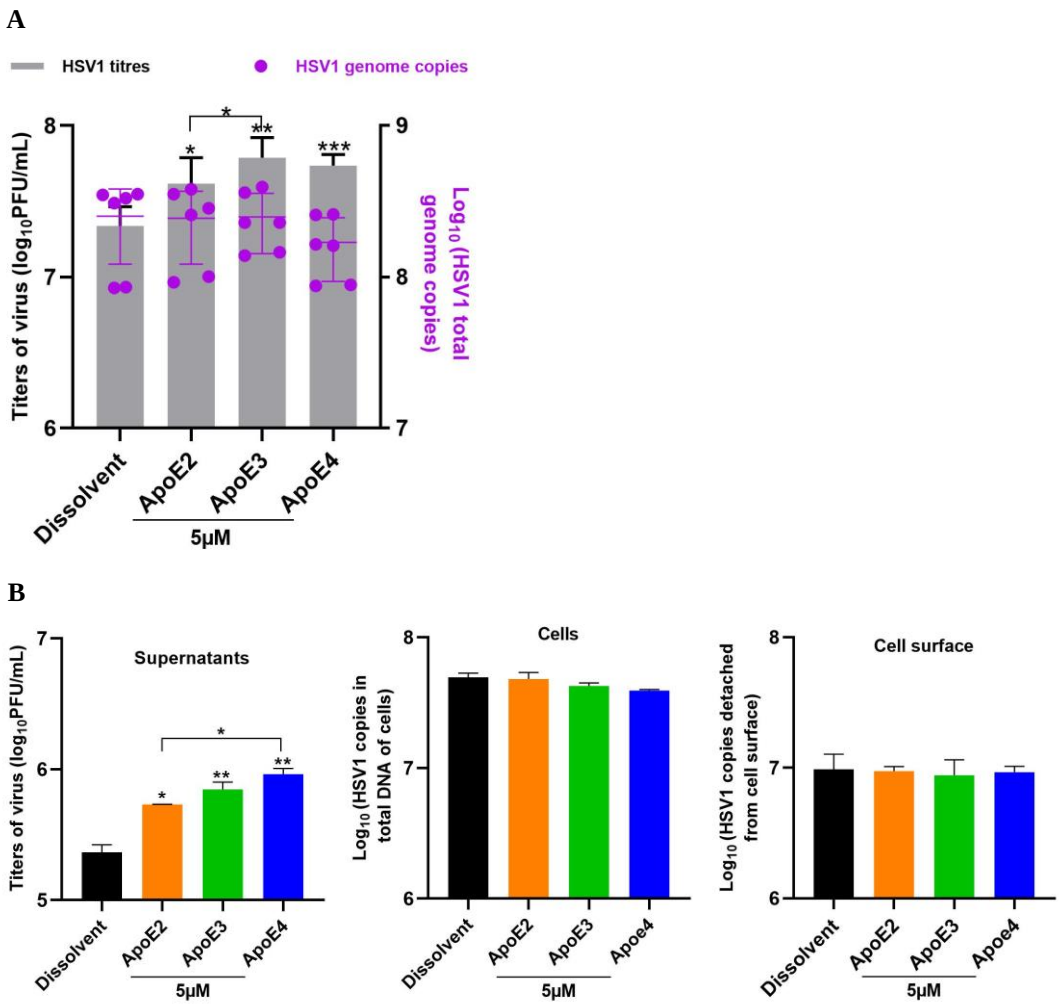

Fig. 3 Replication of HSV1 or the quantity of HSV1 on the cell surface is not affected by ApoE. (A) GMK cells were infected with HSV1 (MOI 0.1) and ApoE or dissolvent was added at 1hpi. At 24 hpi, medium and cell samples of different groups were separated and quantified by plaque assay (grey bars, left Y axis) and qPCR respectively (purple dots, right Y axis). **(B)** Infection was done in the same way as in (A). At 20 hpi, HSV1 on the cell surface was released by trypsin after the separation of supernatants (medium) and cell samples as in (A). Supernatants were quantified by plaque assay; HSV1 released by trypsin or enclosed in cells were quantified by qPCR. Student t-test, ns=not significant, *: $p \leqslant 0.05$, **: $p \leqslant 0.01$.

Next, we quantified the amounts of viruses on the cell surface prior to release. This quantification could be used as an indication for the efficiency of virus assembly and intracellular traffic to the cell membrane. For this purpose, samples were harvested at 20 hpi. After the separation of cells and supernatants, virus particles displayed on the cell surface were released and collected by trypsin digestion. Then the three parts of the sample, i.e, viruses in supernatants, displayed on the cell surface, or enclosed in cells were analysed either by plaque assay or by qPCR. Titration of virus in supernatants revealed ApoE isoform-dependent virus promotions (Fig. 3B, supernatants), consistent with our

previous results. Quantification of cell-associated viruses did not yield significant differences neither in the cell-enclosed nor trypsin-released (cell-surface) materials, suggesting that virus packaging or trafficking is unlikely modified by ApoE (Fig. 3B, cells and cell surface). With more viruses in the supernatant but similar amounts on the surface, our results strongly suggest that HSV1 release from the cell membrane is promoted in the presence of ApoE.

HSV1 detachment from the cell surface is accelerated in the presence of ApoE.

The quantities of HSV1 are similar on cell surfaces of both mock and ApoE treated groups, as shown in Fig. 3C. Taking this as the starting point, we monitored HSV1 release from the cell surface. In this experiment, the supernatant was removed at 20 hpi and the cells were washed with cold PBS. Subsequently, virus release was monitored by harvesting the supernatant at 1h and 2h after washing and quantifying its viral titer by plaque assay. As HSV1 trafficking and release are highly dependent on cellular exocytosis (Griffiths et al., 1985), the experiment was performed on ice, in order to inactivate exocytosis thus excluding the transport of new particles to the cell membrane. Supernatants at 20hpi were titrated as controls before the evaluation of HSV1 release, which confirmed that there were more viruses in the supernatants of ApoE groups at this time point. For both release time points, more viruses were detected in the supernatants from ApoE groups than that of the dissolvent group (Fig. 4), leading to the conclusion that HSV1 detaches faster from the cell surface in the presence of ApoE. As there was no ApoE added in the medium during the release test, we speculate that when HSV1 detaches from the plasma membrane, ApoE is either enriched in the newly produced virus particles or present at the plasma membrane.

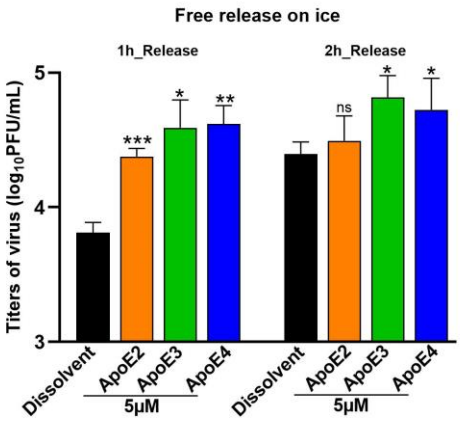

Fig. 4 HSV1 release is promoted by ApoE. GMK cells were infected with HSV1 (MOI 0.1) and ApoE or dissolvent was added at 1 hpi. At 20 hpi, the supernatant was removed and cells were extensively washed with cold PBS. Virus release was monitored for 1 or 2 h and quantified by plaque assay. Student t-test, ns=not significant, *: $p \leqslant 0.05$, **: $p \leqslant 0.01$ and ***: $p \leqslant 0.001$.

ApoE co-sediments with HSV1 particles.

HSV1 has been shown to bind various human lipoprotein particles and artificial proteoliposomes (H.P. Huemer et al., 1988, Intervirology). Recent studies have also revealed that ApoE enriches in virus particles produced from ApoE expressing cells and plays important roles for efficient HBV and HCV infections (Bankwitz et al., 2017; Chang et al., 2007; Jiang & Luo, 2009; Qiao & Luo, 2019). Our results made us wonder whether ApoE was also associated with HSV1 after purification, when such particles are produced from an ApoE expressing cell line. To test this, the ApoE expressing cell line Huh-7, permissive to HSV1 infection, was used. Samples from mock or HSV1 infected groups were separated by ultra-centrifugation through layers of sucrose gradients as described in materials and methods. After centrifugation, samples and sucrose gradients were fractionated from top to bottom and processed for detection of ApoE and HSV1 by western blot. The distribution of ApoE, in the mock or HSV1 infected group, shows different patterns across the sucrose gradients (Fig. 5A and 5B). Without infection, the highest concentration of ApoE was observed in fraction 4, while the concentrations in fractions 1, 2, and 6 were lower and similar (Fig. 5B, ApoE_Mock). In contrast, sedimentation of ApoE through the sucrose gradients was modified after infection: the ApoE concentration was the highest in fraction 1 and gradually decreased through the gradients (Fig. 5B, ApoE_HSV1), which is in a similar trend as that of HSV1-gC (Fig. 5B, gC_HSV1). Titration of the fractionated samples confirmed that the detection of HSV1-gC corresponds with the presence of infectious HSV1 particles (Fig. 5C). The similar distribution patterns of ApoE and HSV1-gC in the infected group strongly indicate that ApoE is hijacked by HSV1 and stays associated with virus particles after release.

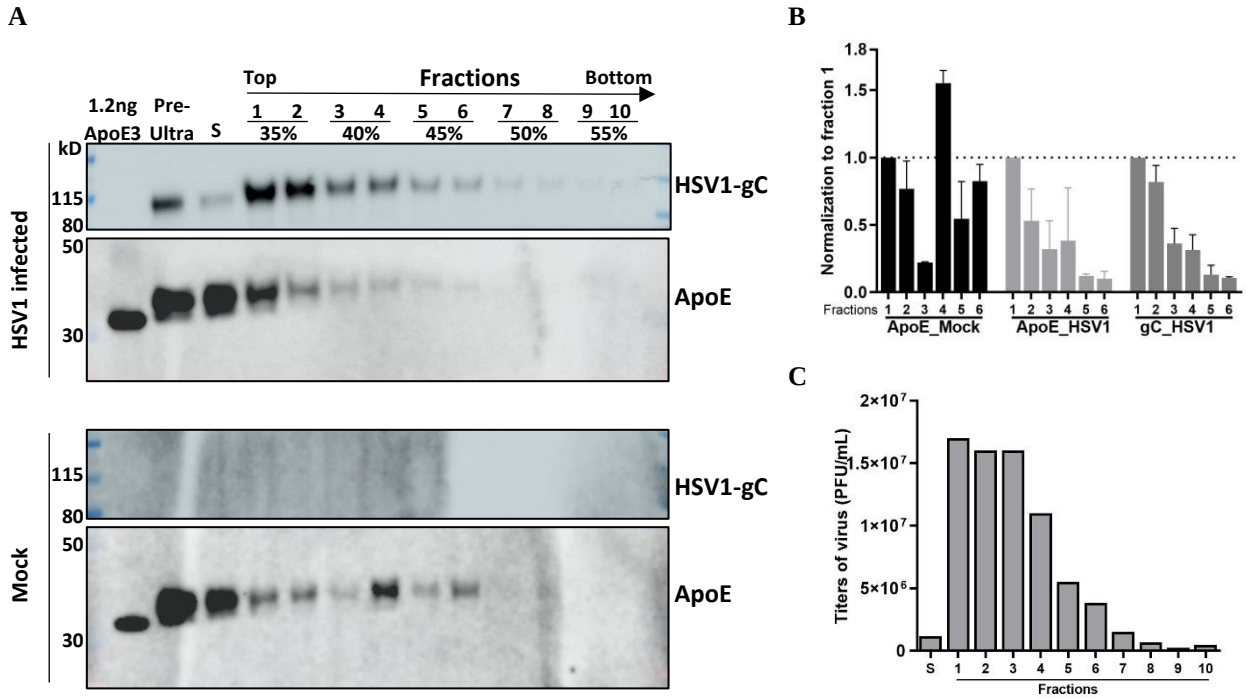

Fig. 5 ApoE co-sediments with HSV1 particles. Huh-7 cells were mock or infected with HSV1 (MOI 0.03) for 72 h. Viruses, proteins, and other contents in the supernatants were concentrated and separated through sucrose gradients by ultra-centrifugation. Samples were fractionated from top to bottom after centrifugation. Solution (S) indicates the samples loaded on top of the sucrose gradients after centrifugation. **(A)** Fractions were analysed by western blot and probed for HSV1-gC and ApoE. Purified ApoE 3 (1.2 ng) was included as a control. **(B)** Distributions of ApoE (of mock or HSV1 infected groups) and HSV1-gC from fractions 1 to 6 were displayed based on the intensities of the corresponding blots from (A). The intensities of different fractions were normalized to the value of fraction 1. Results were generated from two independent repeats. **(C)** HSV1 titres of the corresponding fractions (HSV1 infected groups) were quantified by plaque assays.

Our results are in line with the previously described interactions between HSV1 particles and lipoprotein particles (Huemer et al., 1988). However, if there are interactions between virus particles and purified ApoE protein remains unanswered. To test this, direct interactions were analysed by total internal fluorescence microscopy (TIRFM) visualization of fluorescently labelled HSV1 particles binding to surface-immobilized ApoE. As shown in Fig. 6A, HSV1 binding was dramatically increased when ApoE 4 was present (Fig. 6A, black dots), demonstrating direct interactions between HSV1 and ApoE 4. To further strengthen our results, we tested whether ApoE 4 added exogenously can bind stably to HSV1 particles and thus be co-purified together with HSV1 as complexes after pre-mixing the two. In this case, a purification protocol based on size-exclusion was developed to efficiently remove free protein while recovering intact particles. Western blot analysis of the premixed HSV1 and ApoE 4 confirms that HSV1 is copurified with ApoE 4, indicating that the protein interacts with the virus particles when added exogenously. (Fig. 6B). Lysed HSV1 was included as a control, as the separation is based on the sizes of complexes. In this case, neither HSV1 nor ApoE passed through the purification (Fig. 6B). Finally, it was shown that the binding of ApoE-carrying HSV1 particles to surface-immobilized ApoE 4 was greatly decreased as compared to ApoE 4-free particles further confirming an interaction between HSV1 particles and ApoE 4 (Fig. 6A, blue rectangles). From these results, we conclude that purified ApoE 4 can interact with HSV1 particles, and the complexes formed by ApoE and HSV1 remain stably associated after separation.

ApoE decorated HSV1 demonstrates faster detachment.

The results above raise the question of whether ApoE associated with HSV1 facilitates virus detachment from the cell membrane. To answer this, we characterized the interaction kinetics of HSV1 particles decorated with ApoE or ApoE-free HSV1 particles, to membranes from GMK cells, using TIRFM. For this purpose, native supported lipid bilayers (nSLBs) (Pace et al., 2015; Peerboom et al., 2018), i.e. two-dimensional planar lipid membranes supported onto a sensor substrate and containing plasma membrane material, were used as cell-surface mimetics in biophysical studies of virus membrane interactions. TIRFM allows for the visualization of surface-bound viruses while discriminating them

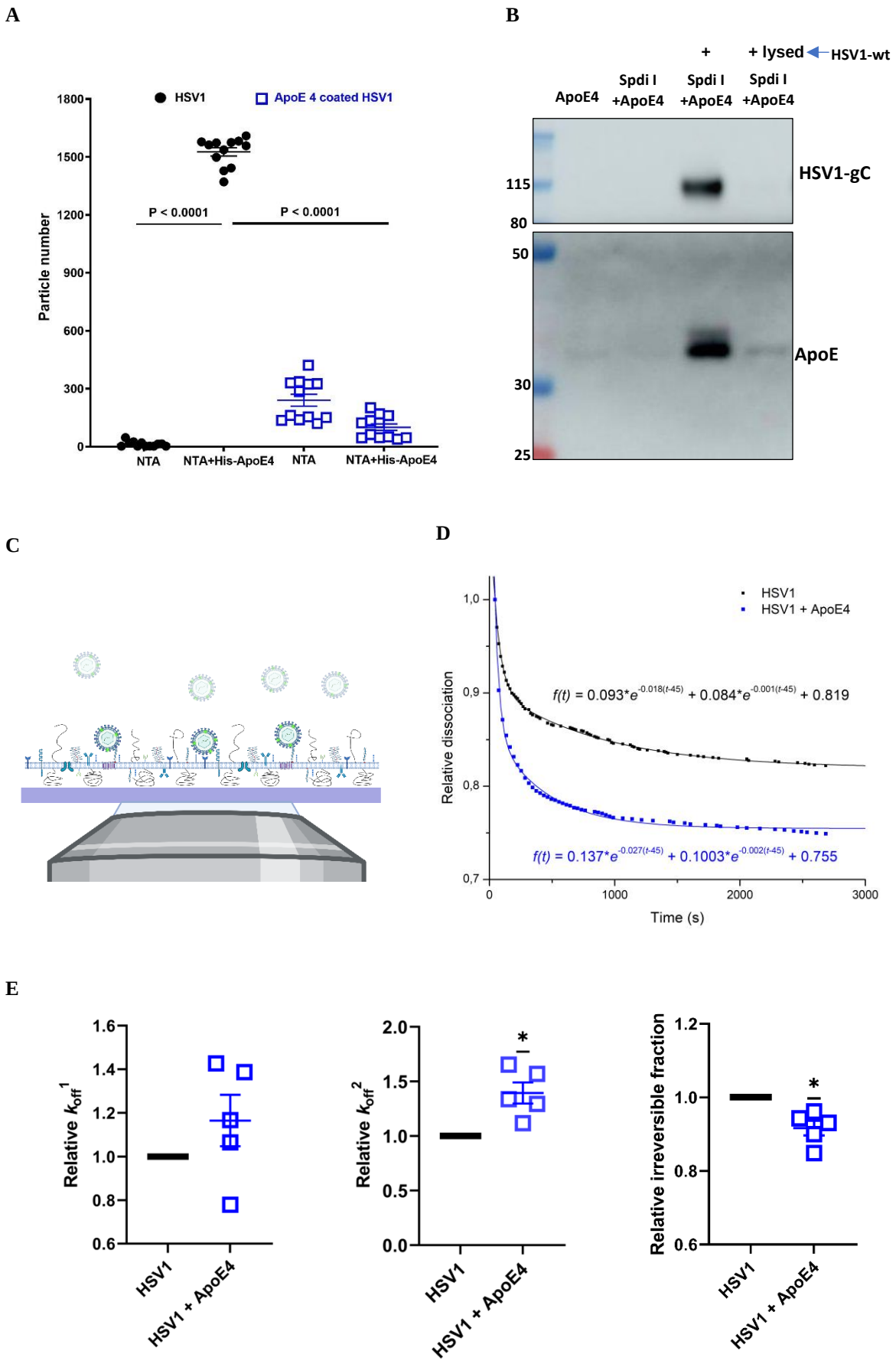
A
HSV1
ApoE 4 coated HSV1
Particle number
1800
1500
1200
900
600
300
0
P < 0.0001
P < 0.0001
NTA
NTA+His-ApoE4
NTA
NTA+His-ApoE4
B
+
+ lysed
HSV1-wt
ApoE4
Spdi I +ApoE4
Spdi I +ApoE4
Spdi I +ApoE4
115
80
50
30
25
HSV1-gC
ApoE
C
D
HSV1
HSV1 + ApoE4
Relative dissociation
1,0
0,9
0,8
0,7
f(t) = 0.093*e^-0.018(t-45) + 0.084*e^-0.001(t-45) + 0.819
f(t) = 0.137*e^-0.027(t-45) + 0.1003*e^-0.002(t-45) + 0.755
0
1000
2000
3000
Time (s)
E
Relative koff1
1.6
1.4
1.2
1.0
0.8
0.6
HSV1
HSV1 + ApoE4
Relative koff2
2.0
1.5
1.0
0.5
0.0
*
HSV1
HSV1 + ApoE4
Relative irreversible fraction
1.2
1.0
0.8
0.6
*
HSV1
HSV1 + ApoE4

Fig. 6 HSV1 particles associate with ApoE 4 and display faster detachment after incubation with purified ApoE 4. (A) Numbers of HSV1 and ApoE 4 coated HSV1 particles on a POPC:DGS-NTA membrane surface with or without His-ApoE 4 immobilized. Each point in the plot represents particle count from a single image of 6 randomly selected fields. Data were produced from 2 independently prepared surfaces. Statistics done by one sample t-test. **(B)** Samples after incubation and purification were lysed and processed for western blot. HSV1-gC and ApoE were probed. **(C)** Schematic image of the nSLB experiments. Planar nSLBs are formed on glass substrate, before being incubated with fluorescent viruses. The interaction between the fluorescent viruses and the nSLB can then be imaged using TIRFM, selectively illuminating only viruses interacting with the surface, while ignoring free viruses in the bulk solution. **(D)** Representative curves of the relative dissociation of HSV1 and ApoE coated HSV1, with corresponding double exponential fits. **(E)** Dissociation kinetics of HSV1 or ApoE-coated HSV1 particles on nSLBs generated from GMK membranes (lacking ApoE). Virus dissociation is plotted over time and fitted with a double exponential function with an offset. Datapoints are 5 individual measurements from three independent experiments. Each datapoint is normalized to its respective HSV control from the same experiment. (Left) Relative k_{off}^1, the fast or (Middle) relative k_{off}^2, the slower dissociation rate constant for ApoE-coated HSV1, normalized to pure HSV1 for each experiment. (Right) Relative irreversibly bound fraction of virus, normalized to pure HSV1 value for each experiment. Error bars indicate mean and standard error of mean. Statistical analysis by one sample t-test with mean 1, *: $p \leq 0.05$.

from the ones in solution (Fig. 6C). This makes it possible to analyze virus-membrane interaction kinetics on a single particle level; information on the dissociation behaviour of the virus from the membrane can be obtained by analysis of the particle residence time, where fitting of the dissociation curves with an exponential function allows for a quantification of the apparent dissociation rate constant (k_{off}) (Fig. 6D) (Peerboom et al., 2018). These experiments revealed that the virus exhibited a heterogeneous detachment behaviour, and that virus dissociation could broadly be separated into two populations characterized by fast (k_{off}^1) or slow (k_{off}^2) dissociation rates. Although no significant difference was observed for the fast dissociation rates (Fig. 6E, left), our results show that the ApoE-decorated HSV1 particles show 39% higher dissociation rates for the slower dissociation compared to HSV1 (Fig. 6E, middle). The ApoE-decorated particles also show an 8,3% reduction of irreversibly bound particles compared to HSV1 (Fig. 6E, right). Combined, these results indicate that ApoE-decoration of HSV1 enhances the dissociation of viral particles from the membranes.

HSV1 particles have similar dissociation rate constants (k_{off}) on membranes with or without ApoE association.

We also hypothesized that HSV1 would detach faster from membranes harbouring ApoE. The residence of ApoE in the plasma membrane, together with caveolin, has been reported in adipocytes (Yue & Mazzone, 2011). Thus, we first tested whether ApoE was also membrane-associated in cells of

relevance to our experiment. For this purpose, an ApoE 4 expression inducible cell line was established. The induction of ApoE 4 expression was verified by western blot (Fig. S2a); and the presence of ApoE 4 was also confirmed in the plasma membrane materials isolated after sucrose purification (Fig. S2b). To compare the influence of membrane-bound ApoE on virus binding kinetics, we produced nSLBs, from both ApoE 4-induced and non-induced cells. Kinetic analysis with TIRFM revealed that HSV1 particles demonstrate a similar dissociation behaviour, when interacting with both ApoE-containing and ApoE-free membranes (Fig. 7). These results indicate that membrane-associated ApoE is not a significant factor in promoting viral release.

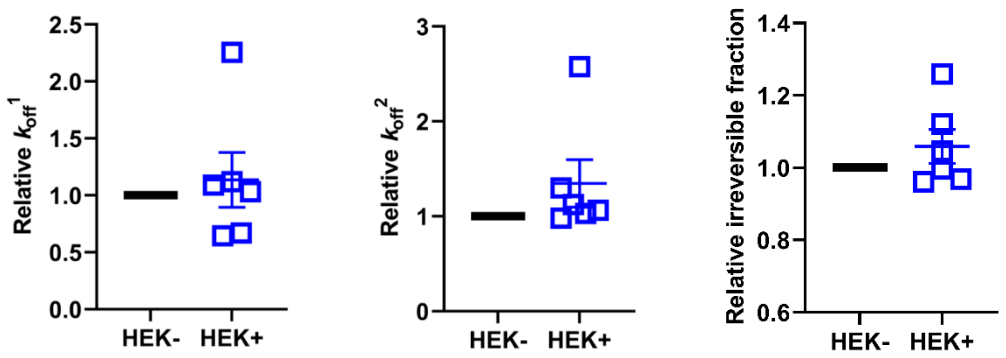

Fig. 7 HSV1 detaches with similar k_{off} on native supported lipid bilayers in the presence or absence of ApoE. Dissociation kinetics of HSV1 particles on nSLBs generated from HEK-ApoE 4 membranes with (HEK+) or without (HEK-) induction of ApoE expression. Virus dissociation is plotted over time and fitted with a double exponential function with an offset. Datapoints are 6 individual measurements from three independent experiments. Each datapoint is normalized to its respective control from the same experiment. After normalization to the values of HEK- for each experiment, the results are presented as relative k_{off}^1 (Left, the faster (larger) dissociation rate constant), relative k_{off}^2 (Middle, the slower (smaller) dissociation rate constant), and relative irreversibly bound fraction of virus (Right). Error bars indicate mean and standard error of mean. Statistical analysis by one sample t-test with mean 1.

Discussion

A number of epidemiological studies have reported that HSV1 infection and ApoE associate with a higher risk of Alzheimer's disease (R. F. Itzhaki et al., 2001; Ruth F. Itzhaki et al., 1997; Lin et al., 1996; Linard et al., 2020; K Lopatko Lindman et al., 2019; Lövheim et al., 2019; Steel & Eslick, 2015; Strandberg et al., 2005). Thus, we were interested in studying potential HSV1-ApoE interactions during virus infection cycles on a molecular level. In this study, we monitored HSV1 growth on cultured cells in the presence of different ApoE isoforms and analysed the effects of ApoE on different stages of the HSV1 infection cycle. Our results demonstrate that ApoE plays an important role in promoting virus detachment from the cell surface upon egress, although it may under certain circumstances, be

detrimental to infection by reducing viral attachment to the cell upon entry. Overall, when grown in the presence of ApoE, HSV1 propagation is promoted, which is attributed to the facilitated release from the plasma membrane by ApoE.

HSV1 attachment is hindered on cells pre-treated with ApoE (Fig. 2A). This inhibition is likely due to the occupancy of heparan sulfate (HS) on the cell surface by ApoE, as HS is a known receptor for both ApoE (Saito et al., 2003) and HSV1 (Shieh et al., 1992). Binding to HS is predominantly mediated by a domain located at the N-terminal of ApoE (136 – 147) (Libeu et al., 2001). As expected, Dobson and colleagues have shown that dimers of a peptide (141– 149aa) derived from this domain clearly inhibit virus attachment and subsequent infection of different viruses including HSV1 and HSV2 (Dobson et al., 2006). However, the full-length ApoE failed to show inhibition to HSV1 attachment and infection in their studies, even at a concentration of 11.2 μM (Dobson et al., 2006), while our results revealed inhibition of HSV1 attachment with 5 μM of full-length ApoE. Such a difference could be explained by the different experimental designs: in Dobson's study, ApoE was added to cells at the same time as HSV1, for only 1h inoculation then removed thereafter, which is different from our experiments where ApoE was added to cells 4 h prior to HSV1 infection. Such experiments indicate that the pre-treatment of the cells with ApoE could give ApoE some advantages to occupy HS on the cell surface, thus resulting in a reduction of HSV1 binding. In fact, we have also conducted an experiment using a similar experimental procedure to Dobson's where ApoE (50 nM, 500 nM, or 5 μM) was first incubated for 1 h with HSV1 at 37 °C followed by a 1 h inoculation on cells, but not refreshed thereafter. The results show that HSV1 grow similar in all groups (data not shown), which is in line with Dobson's observation for the full-length ApoE (Dobson et al., 2006). In the case of ApoE dimers, the inhibitions to virus infection were only effective at high concentrations (>15 μM) (Dobson et al., 2006). We speculate that high concentrations of ApoE or adding ApoE before HSV1 infection is required to reduce HSV1 attachment to HS. Yet our results demonstrated that under certain conditions, ApoE can interfere with HSV1 binding at the cell surface.

We have also observed in our experiments that inhibition of HSV1 attachment by ApoE is isoform dependent, with similar inhibition effects for ApoE 3 and 4, but weaker for ApoE 2 (Fig. 2A). The binding affinities of ApoE to heparin, a secreted highly sulphated version of HS, commonly used as a surrogate to HS in in vitro studies, vary among different isoforms: ApoE 4 and 3 have similar affinities which are higher than ApoE 2 (Futamura et al., 2005). Thus, there are good correlations between the inhibitory abilities of ApoE to HSV1 binding and the protein's affinities to HS, adding more evidence that the binding inhibition to HSV1 is a consequence of occupying HS by ApoE. Although ApoE can inhibit HSV1 attachment, this inhibition is thought to play minor roles in our experiments. In the experiments where ApoE was added after 1h inoculation with both single (MOI 10) and multiple (MOI 0.1) infection cycles, the effects of ApoE on virus binding during the first infection cycle is negligible, considering that HSV1 binding and entry can be mostly completed within 30 min (Nicola & Straus,

2004). During the tests with multiple HSV1 infection cycles, we postulate that binding inhibition by ApoE is unlikely present after the first infection cycle, as the concentrations of ApoE would have reduced due to its degradation (Ladu et al., 2006; Ye et al., 1993). In fact, when infection initiated after overnight incubation of ApoE on cells, HSV1 growth was promoted similarly as when ApoE was added after 1h inoculation (Fig. S1b), providing a hint that binding inhibition of ApoE is negligible after overnight incubation.

The release of HSV describes the detachment of viral particles from the cell surface, which is the final step of virus infection cycles during its cell-free transmission. In general, this process is much less studied in comparison to other steps. Several studies on this topic have pointed to the effects of viral proteins and/or host factors on virus release. In the context of viral proteins, ICP27 of HSV1 was found to be important to virus release, as a replacement of HSV1 ICP27 with the HSV2 version resulted in more viruses detained on cell surface, thus less released viruses in the medium (Park et al., 2015). Nevertheless, most studies stress that efficient HSV release relies on fine-tuning and overcoming the interactions between viral proteins and GAGs on cell surface. Indeed, studies focusing on the release of HSV1 or HSV2 have shown that highly o-glycosylated domains of viral proteins, so called mucin-like domains, play a key role in modulating virus-GAG interactions. Accordingly, virus mutants, lacking either the mucin-like domain on the viral glycoprotein gC, in the case of HSV-1 (Altgärde et al., 2015) or lacking the mucin-like membrane-associated glycoprotein G in the case of HSV-2 (Edward Trybala et al., 2021), demonstrated deficiency in virus release. Such release deficiencies of both HSV1 and HSV2 could be rescued by exogenously adding heparan sulfate or similar molecules (Altgärde et al., 2015; O'Keeffe et al., 1998; Edward Trybala et al., 2021). Along the same line, elevated heparinase expression was also shown to promote the release of HSV (S. R. Hadigal et al., 2015; Hopkins et al., 2018a). All these results illustrate that modifications of the virus-GAGs interactions can modify virus release, which leads us to speculate that ApoE may influence HSV1 release, by acting as a modulator of virus-GAG interactions. Indeed, our new results reveal that the host factor ApoE can promote HSV1 release from the cell surface, with stronger promotions by ApoE 3 or 4 than that by ApoE 2 (Fig. 4). This isoform-dependent effects correlate with their binding affinities to heparin. Thus, the results suggest that the promotion of HSV1 detachment by ApoE is attributed to potential manipulations of HSV1- HS interactions. Different to the observations from studies of ICP27, our results show that prior to the final release, the amounts of virus particles displayed on cell surface are not affected by ApoE, while more HSV1 were released in the medium. We speculate that HSV1 detachment kinetics reach a new equilibrium in the presence of ApoE. This is supported by our kinetic studies of HSV1 on nSLBs where we compared the influence of particle-associated ApoE and observed faster release of ApoE-coated HSV1 (Fig. 6D & E).

Alpha herpesvirus particles are transported in membrane vesicles (reviewed in (Ahmad & Wilson, 2020)) to specific sites on the cell surface (Hogue et al., 2014; Mingo et al., 2012) via cellular exocytosis

pathways. The actual delivery is completed via membrane fusion between the virus-containing vesicles and the cell plasma membrane. It is unknown whether the final release happens at the same sites where virus particles become exocellular or at different sites which requires lateral movement/transport of extracellularly exposed virus particles from the membrane fusion sites. Nevertheless, HS can be involved in the final detachment at either of the release sites. This means that potential interventions to the HSV1-HS binding from ApoE or other HS ligands should occur at the actual virus release sites. With this assumption, hijacking ApoE by the virus would be a smarter solution to localize proper amounts of ApoE at the release site than having ApoE homogeneously distributed in the plasma membrane. This may explain why we have observed improved virus detachment with ApoE coated HSV1 (Fig. 6D & E), but not for non-coated HSV1 on nSLBs harbouring ApoE (Fig. 7). It is worth mentioning that the nSBLs were generated from non-infected cell materials (HEK or HEK-ApoE). Thus, our tests cannot exclude the possibility that virus infection modifies and re-arranges membrane association of ApoE in a way that facilitates final release.

Direct biomolecular interactions between ApoE and HSV1 have been observed in our studies, which are supported by two sets of data generated using different methods: co-sedimentation of ApoE and HSV1 after ultracentrifugation (Fig. 5); and purification of ApoE associated HSV1 after incubation (Fig. 6A and B). These results are also complementary to a previous study where interactions were reported between HSV1 and purified serum lipoparticles or artificial proteoliposomes harbouring apolipoproteins, including ApoE (Huemer et al., 1988). An interesting question is what mediates the interactions between ApoE and HSV1 particles. Samples for sedimentation analysis were generated from HSV1 infection on live cells, which suggests that the interactions between ApoE and HSV1 could take place at any stage of the infection cycle. While co-purification of complexes formed with purified HSV1 and ApoE 4 points out that ApoE can interact and remain associated with intact and mature virus particles. Such interactions are likely mediated by viral component(s) on the surface of virus particles, e.g, viral glycoproteins. From our attempt, we have excluded potential interactions between ApoE and some HSV1 glycoproteins, including glycoprotein B, C, D, and E, by immunoprecipitation test (data not shown). These results indicate that other glycoproteins should be investigated as potential ApoE interaction partners in future studies.

Incorporation of ApoE into virus particles has also been reported for HBV and HCV (Gastaminza et al., 2010; Qiao & Luo, 2019), but to the best of our knowledge not previously for HSV1. The roles of ApoE during HBV or HCV infection seem to be different to those of HSV1 revealed from our study. During infection of HBV or HCV, ApoE has been suggested to be involved in virus attachment by working as a bridge ligand between virus and cell surface receptors, including HS (Jiang et al., 2013; Li & Luo, 2021; Xu et al., 2015); the virus itself lacks HS-binding capacity. This is in contrast to the HSV1 case which has several HS-binding glycoproteins, including gC (Altgärde et al., 2015; Herold et al., 1991). This suggests that ApoE negligibly interferes virus binding to HS. In addition to virus attachment to

HS, several studies suggest that ApoE is also involved in the late steps of HCV infection (Bankwitz et al., 2017; Benga et al., 2010; Cun et al., 2010; Lee et al., 2014). Whether HCV release is affected by ApoE is unknown. The participation of ApoE at late steps of HCV infection may be different from that for HSV1 seen in our studies, as HCV growth benefits similarly from all three ApoE isoforms (Cun et al., 2010).

ApoE is an important host protein which is involved in infections of different viruses. Our results reveal novel roles of ApoE during HSV1 infection at molecular levels, and some isoform dependent effects. However, the significance of ApoE and HSV1 interactions in AD development remains to be studied. Especially, other factors such as amyloid-beta and tau protein should be considered when studying the development of the disease. In addition, considering the limitations of data generated from immortalized cell culture, more comprehensive models, such as recently developed brain organoids (Bi et al., 2021; Martens et al., 2021), are suggested for a deeper study of ApoE and HSV1 interactions, as well as their significance in disease development.

Materials and method

Cells and ApoE proteins

Both green monkey kidney (GMK AH-1) and neuroblastoma SH-SY5Y (CRL-2266) cells were purchased from ATCC, and kindly provided by Tomas Bergström (Gothenburg University) and Niklas Arnberg group (Umeå University), respectively. A hepatocyte-derived carcinoma cell line (Huh-7) was a gift from Magnus Evander (Umeå University). GMK cells were cultured in DMEM (D5648-10L, Sigma), supplemented with 10% fetal bovine serum (FBS, SV30160.03, cytiva), 20 mM HEPES, penicillin (0.5 unit/mL) and streptomycin (50 µg/mL) (P0718, Gibco). SH-SY5Y cells were cultured in a mixture of medium with 1:1 DMEM + F-12 HAM (21700-075, Gibco), 10% FBS, 20 mM HEPES, penicillin (0.5 unit/mL) and streptomycin (50 µg/mL). The ApoE 4 inducible cell line was established by using the Flp-In ™ T-Rex ™ system (a kind gift from Anna Överby group, Umeå university), according to the manufacturer's instructions (Invitrogen). In brief, the ApoE 4 gene was synthesized and verified by the Protein Expression Platform at Umeå university, and then constructed in the backbone of pcDNA™5/FRT/TO expression vector. Together with a recombinase expressing vector pOG44, pcDNA™5/FRT/TO-ApoE 4 was co-transfected into a commercially established Flp-In™-293 cell line carrying the integrated FRT. After transfection, selection for successful gene integration was done under hygromycin (100 µg/mL). The ApoE 4 inducible cell line was derived from a single clone and the induction of ApoE 4 expression by tetracycline (1 µg/mL) was verified by western blot. Cell cultures were maintained 37°C and 5% CO_2 in an incubator. ApoE protein was produced and purified in Anders Olofsson's lab. Lyophilised ApoE proteins was first dissolved in 20 mM NaOH and then

mixed with 10× PBS (volume ratio of 20 mM NaOH and 10× PBS is 9:1)) to make the stock solution at a concentration of 50 µM (= 1.7 mg/mL). ApoE protein solutions were aliquoted and kept at -80°C. The dilution buffer alone was used in control experiments, termed as the dissolvent group. All protein aliquots used for experiments experienced no more than two freeze-thaw cycles, to minimise variations in protein concentrations.

Viruses and virus purification

Herpes simplex virus 1 (HSV-1) strain KOS (VR-1493; ATCC, Manassas, VA) was produced and purified in our lab by ultracentrifugation through sucrose gradients (Marconi & Manservigi, 2014). In brief, propagation started with MOI 0.01 infection of GMK cells. Viruses from both cells and medium were collected, concentrated, and loaded on sucrose gradients (consist of 2 mL each of 50%, 40%, 30% sucrose layers, w/v) for purification. Cell-associated viruses were released by three freeze-thaw cycles. After centrifugation at 20200 rpm for 2 h, virus particles sediment at the interface between the 50% and 40% sucrose layers. After collection of the virus-containing fraction, viruses were aliquoted in sucrose for infection studies on cultured cells. For biophysical experiments, sucrose was exchanged with PBS by an extra round of high-speed centrifugation (48384 g, 20 min at 4°C).

Quantification of virus binding

Virus binding quantification by qPCR was done in 12-well plates. Prior to adding viruses, cells were treated with ApoE for 4 h. 200 PFUs/well of virus diluted in 150 µL infection medium (DMEM, 1% FBS, 20 mM HEPES, and 1% Penicilline and Streptomycin) was added for infection. Virus binding synchronization was also done on ice while rocking the plate every 10 min for 1 h. Unbound viruses in the solutions were removed and cells were quickly washed with PBS twice. The attached viruses were harvested together with cells for DNA extraction according to the manufacturer's instruction (Invisob Spin Virus DNA Mini Kit, IBL). Virus DNA was quantified with primers targeting the US5 (unique short 5) (Filén et al., 2004) gene as previously described (Abidine et al., 2022). A standard curve established with pI18-HSV1-US5 as the template was used to calculate the absolute quantities of HSV1 copies. The two primers used for qPCR were: HSV1-US5-F, (5'-GGCCTGGCTATCCGGAGA-3'); HSV1-US5-R (5'-GCGCAGAGACATCGCGA-3'). The probe for qPCR was 5'-6FAM-CAGCACACGACTTGGCGTTCTGTGT-Dark Quencher-3'. The qPCR program run as 95°C, 3 min; 40 cycles (95°C, 15 s; 60°C, 30 s). Since the concentration of virus (200 PFUs) was too low for stable detection via qPCR, binding quantification was achieved after increasing the amounts of viruses to 5,000 PFUs and 25,000 PFUs. Quantification of different PFUs as inputs by qPCR revealed an almost perfect linear regression (Abidine et al., 2022), confirming that this approach was viable.

Viral entry efficiency assay

Virus entry efficiencies were investigated by a previously described method (Abidine et al., 2022). Before the entry assay, virus binding was done in the same way as in binding quantification. Thereafter, viruses attached to the cell surface were either inactivated immediately (t=0 min) by low pH buffer (pH=3, 40 mM citric acid, 10 mM KCl, 135 mM NaCl) (Desai et al., 1988; Nicola & Straus, 2004) or shifted to 37°C for active entry for selected periods of times (t=10, 20, 30, 60 and 90 min) before low pH buffer inactivation. Low pH buffer inactivation was done by adding 350 µL/well of low pH buffer for 2 min on ice, shaking every 20 – 30 s, followed by two PBS washes. After inactivation of the uninternalized virus, cells were covered by 1% agarose in DMEM (5% FBS) for another 3 days culture until obvious plaque formations. A low MOI was chosen to ensure a clear readout of plaque formation. Cells were then fixed with 4% formaldehyde (in PBS) and stained with crystal violet (1% crystal violet in 20% ethanol solution). The number of plaques was then counted for each condition. The quantification of the virus entry efficiency was then done by dividing the number of plaques by their corresponding binding factors (binding ratios normalized to the dissolvent group, Fig. 2A).

Quantification of cell-associated virus

To quantify the total amount of cell-associated viruses, infected cells were harvested separately from the medium for DNA extraction and subsequent qPCR quantification of viral genome copies. To specifically quantify virus particles on the cell surface, viruses were released by trypsin and separated from cells by centrifugation. Experiments were carried out in 12-well plates. At indicated time points after infection, medium samples were harvested for titration by plaque assay. Cells were then washed with PBS twice, followed by trypsin addition. After trypsin digestion, cells were resuspended in PBS and collected for centrifugation at 1500 rpm for 5 min. After centrifugation, cells and supernatants were separated. Released viruses in supernatants and intracellular viruses were then processed for DNA extraction and genome quantification by qPCR.

Quantification of virus release rate from infected cells

The release rate of virus was investigated in the premise that similar amounts of viruses were found on the cell surface (Fig. 3B) in all groups at the indicated starting time point. The virus release into the medium (Fig. 4, without refreshing of any ApoE) was then monitored for 1 or 2 h. Released viruses were later quantified by plaque assay.

Co-sedimentation, SDS-page, and western blot

Co-sedimentation analysis of HSV1 and ApoE was done in a similar procedure as for the virus production and purification described above. Medium of HSV1-infected Huh-7 cells (only released HSV1) or mock was collected and concentrated, followed by separation by ultracentrifugation through sucrose gradients (consist of 2 mL each of 55%, 50%, 45%, 40%, 35% sucrose layers, w/v). After centrifugation, samples loaded on top of the sucrose gradients were harvested as one fraction, termed

as “solution (S)”. Samples in sucrose gradients were fractioned from top to bottom (1 mL/fraction). Samples from each fraction were processed for SDS-page and western blot for detection of ApoE protein (PA5-27088, Invitrogen, diluted in 5% milk in PBS-tween) and HSV1-gC (B1C1B4, diluted in 5% milk in PBS-tween) (Delguste et al., 2019). In brief, samples for SDS-page and western blot were lysed in lysis buffer (0.05 M Tris-HCl pH=8, 0.15 M NaCl, 1% Triton X-100, in H_2O + protease inhibitor cocktails (Roche)) for 15 min on ice, followed by centrifugation at 12000 rpm for 15 min, at 4°C. The supernatants were collected, and aliquots were mixed with 6x laemmli buffer then boiled at 95°C for 10 min. Boiled samples were quickly cooled down on ice and used for SDS-page. Intensities of ApoE and HSV1-gC bands were analysed by ImageJ (Schindelin et al., 2012). Titers of the corresponding fractions were quantified by plaque assay for their infectivity.

Purified HSV1 and ApoE 4 incubation, complex separation, and fluorescence labelling

Incubation and fluorescence labelling of purified HSV1 and ApoE 4 protein was done at the same time for the experiments described in Fig. 6. 2×10^8 PFU HSV1, 8µL ApoE (50 µM in stock), and 1µLfluorescent lipophilic dye 1,1’-dioctadecyl-6,6’- di(4-sulfophenyl)-3,3, 3’,3’-tetramethylindocarbocyanine (SP-DiIC18(3)) (D7777, Invitrogen, 400 µM in stock) were added in a 1.5 mL Eppendorf tube. The mixtures were incubated under rotation for 1 h at room temperature, followed by adding 100 µL/sample Capto-core beads (Capto Core 700, 17548101, cytiva) to the same tube and a further 1h incubation at 4°C. Capto-core beads were separated by centrifugation at 800 g, 2 min. The supernatants were collected and further purified by running through S-200 columns (MicroSpin^{TM}S-200 HR Columns, 27512001, cytiva). In parallel, HSV1 without ApoE 4 added, was included as a control for comparison in the designated experiments. When HSV1 without ApoE incubation was used for kinetic analysis (Fig. 7), 2×10^8 PFU virus was freshly labelled prior to each experiment with 2 µL of fluorescent lipophilic dye 3,3'-Dioctadecyl-5,5'-Di(4-Sulfophenyl) Oxacarbocyanine, Sodium Salt (SP-DiOC18 (3)) (D7778, Invitrogen, , 400 µM in stock), followed by size exclusion and buffer exchange by filtration through MicroSpin S-200 HR columns (27-5120-01, cytiva,) (N. Peerboom, et al., 2017, Biophs. J.; N. Peerboom, et al., 2018, ACS Infect. Dis). After labelling, lost viruses were estimated to 60% using a Förster Resonance Energy Transfer (FRET)-based assay (Thorsteinsson et al., 2020).

Small Unilamellar Vesicles for (native) supported lipid bilayers.

1-palmitoyl-2-oleoyl-glycero-3-phosphocholine (POPC) (850457P), 1,2-dioleoyl-sn-glycero-3-[(N-(5-amino-1-carboxypentyl) iminodiacetic acid) succinyl] (18:1 DGS-NTA(Ni)) (790528P), and N-palmitoyl-sphingosine-1-{succinyl[methoxy(polyethylene glycol)5000]} (PEG) (880280P) were purchased from Avanti Polar Lipids (Alabaster, AL, USA). 1,2-dihexadecanoyl-sn-glycero-3-3phosphoethanolamine, triethylammonium salt (TxRed) was purchased from ThermoFisher Scientific (T1395MP). Small unilamellar vesicles (SUVs) were prepared by extrusion using a mini extruder

equipped with 1 mL syringe (610020 and 610017; Avanti Polar Lipids) as described previously (Peerboom et al., 2017). Pure POPC vesicles, POPC:PEG vesicles (99.5:0.5, molar ratio), and POPC:TxRed vesicles (99:1, molar ratio) were all prepared in PBS by extrusion through a 100 nm polycarbonate membrane at least 11 times. POPC:TxRed was prepared at a stock concentration of 4 mg/mL, the others at 1 mg/mL. POPC:DGS-NTA vesicles (96:4, molar ratio) were prepared in HEPES saline buffer (HBS, 10 mM HEPES and 150 mM NaCl; pH 7.5) at a stock concentration of 1 mg/mL by extrusion through a 50 nm polycarbonate membrane at least 21 times and were stored under N_2 . All stocks were stored at 4°C.

Binding assay of HSV1 to surface immobilised His-tagged ApoE.

Borosilicate glass cover slides with a diameter of 22 mm (631-0158P, round, No.1, VWR) were cleaned using 7x detergent (MP Biomedicals, CA) and milli-Q water with 1:6 (volume ratio) solution close to boil for 2 h, rinsed extensively and stored in milli-Q water. Before use, the slides were rinsed with milli-Q water, N_2 dried, and treated in UV/ozone (UV Ozone Cleaner -ProCleaner™ Plus, Bioforce, IA, USA) for 30 min.

Supported lipid bilayers (SLBs) were formed from SUVs by the method of vesicles spreading, through 30 min exposure of 50 µg/mL vesicle solution in HBS supplemented with 10 mM $NiCl_2$ to freshly cleaned glass cover slip. The cover slip was fixed on a custom Teflon holder using a bi-component Twinsil glue (Picodent, Germany), creating eight wells of equal volume. All incubation steps were performed in still solution. The excessive SUV material was removed from each well by rinsing 20 times with100 µL PBS. After rinsing, SLBs were incubated with POPC vesicles for 30 min at final concentration of 37.5 µg/mL to ensure the formation of a good quality bilayer by filling up any potential gaps. After rinsing in PBS, six wells were exposed to His-tagged ApoE 4 at a final concentration of 100 µg/mL for 30 min. Wells that were not exposed to His-tagged ApoE 4 were used as control. After rinsing with PBS, six wells were exposed for 30 min to fluorescently labelled HSV1 particles with or without preincubation with ApoE 4 (see purified HSV1 and ApoE incubation section for details). Images (704 x 704 pixels with a 0.183 µm pixel width) of bound particles at six randomly selected positions were collected using total internal reflection fluorescence (TIRF) microscopy with an inverted Nikon (Japan) Eclipse Ti-E2 microscope. The images were analysed using ImageJ. A Gaussian blur (sigma:1 pixel) was applied to all images to reduce the noise and particles were counted after thresholding. Raw particle number were normalized between samples to account for differences in the stock concentration. Experiments were repeated twice.

Determination of the relative concentrations of fluorescently labelled HSV1 samples.

The concentration of labelled particles in each sample was calculated using an assay referred to as "bouncing particle analysis". In brief, this method measures the number of particles that transiently diffuse close to the glass surface into the TIRF excitation volume without interacting with the substrate,

i.e., “bouncing” off the surface. Since particles randomly diffuse in the solution, the number of particles detected during this procedure is linearly proportional to the particle concentration in solution. The measurement was performed on pure POPC SLBs, which are resistant to HSV1 attachment, to minimise the interaction between the particle and the substrate. The timelapses were recorded in TIRF mode using a laser (TO BE ADDED) with 565 nm wavelength at 50% power and at 10 fps for 1min. The movies were analysed using an in-house MATLAB (MathWorks, USA) script using the same principle as described for the kinetic analysis (see section Virus binding kinetics). Only particles detected on the surface for less than 10 frames or 1s were considered non-interacting with the substrate and counted as “bouncing particle” events. The cumulative sum of new bouncing particles was then calculated versus time and fit to determine the rate of arrival (slope of the cumulative sum). This factor is linearly proportional to the particle concentration in solution and was used to normalize the concentrations across samples.

For both samples, movies were recorded at three different randomly selected positions, analysed, and averaged to extract the arrival rate. From this analysis, the naked HSV1 sample was observed to be 1.1 times more concentrated than the ApoE 4-coated HSV1 sample.

Membrane extraction and purification

Native membrane vesicles (NMVs) were prepared according to a protocol adapted from Pace et al. (Pace et al., 2015). Confluent cells were rinsed with cold PBS, and then harvested on ice in ice-cold harvest buffer (PBS mixed with EDTA-free protease inhibitor cocktail, Roche) using a cell scraper. Harvested cells were pelleted via centrifugation at 600 g for 10 min, before they were disrupted using a CF1 continuous flow cell disruptor (Constant Systems, U.K.). The suspension was then centrifuged at 2,000 g for 10 min to pellet nuclei and larger organelles, and then at 6,000 g for 20 min to pellet mitochondria. Finally, the suspension was centrifuged at 150,000 g for 90 min to pellet the NMVs.

NMV pellets were resuspended in harvest buffer and purified via sucrose gradient, to separate plasma membrane vesicles from organelle membrane vesicles. The suspension was mixed with equal volume of 80% sucrose solution, and then layered with a 30% and 5% sucrose solution respectively. All sucrose solutions were made with harvest buffer. The sucrose cushion was then centrifuged at 273,000 g for 2.5 h. The NMVs form a clear band at the 5 - 30% sucrose interface, which was harvested, flash-frozen, and stored at -80°C. All centrifugations were done at 4°C.

Concentration of NMV material was measured using a FRET based assay described previously (Thorsteinsson et al., 2020).

Native supported bilayer preparation

Native vesicles were mixed with synthetic POPC:PEG vesicles in a 15:85 % ratio, according to the surface area determined with the FRET assay (Thorsteinsson et al., 2020). Mixing was done in 1.5 mL

microcentrifuge tubes (Eppendorf) for a final concentration of 200 µg/mL and a final volume of 60 µL. The mixture was sonicated for 20 min at 40°C in a bath sonicator (37 kHz, Elmasonic S40H, Germany). After sonication, vesicles were then mixed with 0.3 µL of 0.5 µg/mL POPC:TxRed vesicles.

Borosilicate glass cover slides with diameter of 24 mm (631-0161, round, No.1, VWR) were cleaned using 7x as described above, but without UV-ozone treatment. Bilayers were formed in custom-made 10 µL PDMS wells attached to the cover slides. 10 µL of vesicle mixture was injected into wells and incubated for 30 min at 37°C. Afterwards, wells were rinsed 10x with 10 µL PBS, before passivating the bilayer with POPC vesicles at a final concentration of 50 µg/mL. Bilayers were then visually inspected for unruptured POPC:TxRed vesicles to confirm bilayer formation before proceeding.

Virus binding kinetics.

Kinetic timelapses were imaged with the Nikon Ti-E2 microscope in TIRF mode. Fluorescently labeled virus particles were incubated with nSLBs for 1 hour before recording kinetics at either 15 (data in Fig. 6) or 30 seconds/frame (data in Fig. 7) for 361 frames. Timelapse field-of-view is 704 x 704 pixels with a resolution of 0.183 µm/pixel.

Movies were stabilised using an in-house MATLAB script. The MATLAB script takes as reference image the first frame and performs an image registration based on maximising the cross correlation between the current and reference frame. The reference frame is updated after one third of the length of the movie to improve the registration of rapidly changing videos. In the case a shift larger than 15 pixels in any direction is detected, the script updates the reference frame to the last analysed frame and repeats the registration. If no improvement is observed, a more computationally intensive multimodal registration algorithm is attempted. In the case of low density of particles, the script average over all the frames and crops the field of view to only consider the area presenting the 10 brightest spots to reduce possible errors in the correlation calculation due to random noise. Only rigid translation is considered in every case.

We then analysed the stabilised movies for kinetic analysis using an in-house MATLAB script with improved detection capabilities from what previously described (Peerboom et al., 2017). In brief, in each frame, particles are detected by performing two successive 2D peak scan. Firstly, peaks of prominence higher than a threshold set by the user are identified as particles. The threshold is then lowered by a percentage set by the user and newly detected peaks are considered only if a particle was also detected in the proximity in the previous frame. This is to account for possible bleaching in long exposure experiment which might reduce the intensity of particle on the surface below the higher threshold. The same thresholds were used for all samples for the same experiments. A nearest neighbour algorithm is then used for linking the particle by comparing successive frames with a maximum linking distance of 2 pixels. Possible errors in linking causing the fragmentation of single tracks, thus false attachment, and detachment events, are corrected by comparing the position of tracks ending and

beginning in successive frames and linking them if within 1 pixel. Finally, detachment events causing an intensity drop lower than three times the standard deviation of the background are discarded.

For the kinetic analysis, a particle was considered bound if it remained on the surface for at least three consecutive frames. The particle dissociation rate was quantified by plotting the number of bound particles as a function of the residence time on the surface and fitting the curve with a double exponential function with an offset. Only particles that bind during the first half of the timelapse were included in the analysis, to avoid biasing the data towards shorter residence times.

Supplement figures

Fig. S1

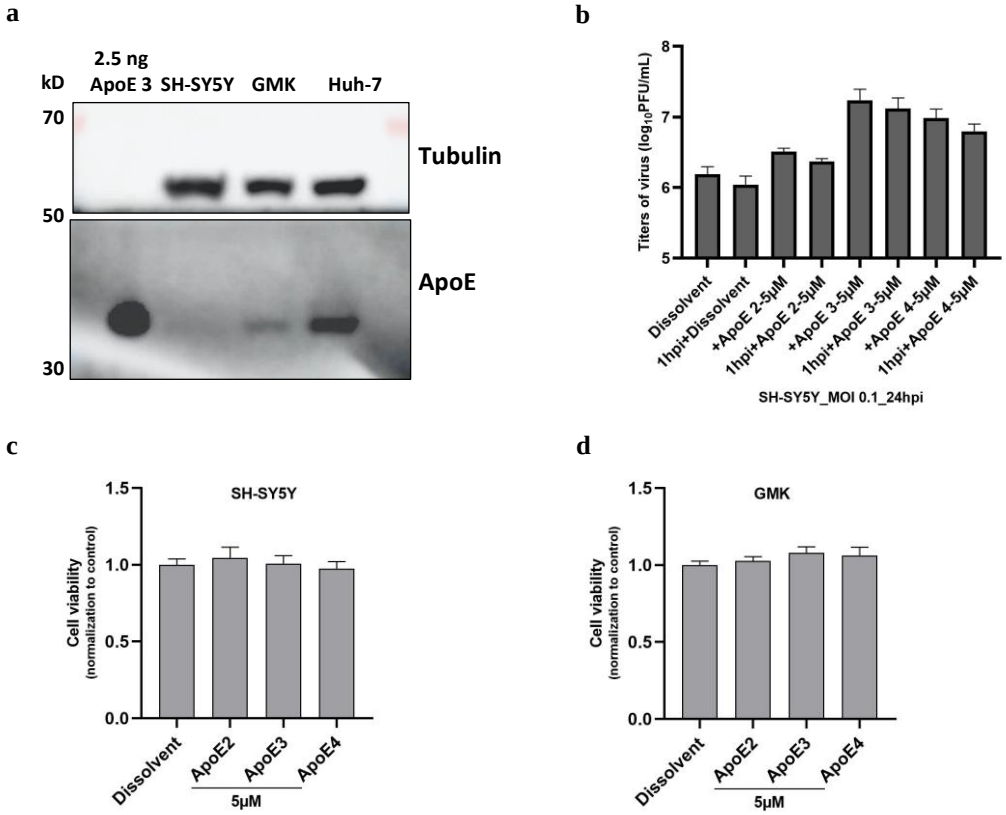

Fig. S1: **(a)** Same amounts of SH-SY5Y, GMK, or Huh-7 cells were lysed and analysed by western blot for ApoE expression. Tubulin and ApoE were probed. **(b)** HSV1 growth was analysed by plaque assay after infection of SH-SY5Y, where 5μM ApoE was either pre-incubated overnight (labelled as +ApoE) or added after 1h virus inoculation (labelled as 1hpi + ApoE). SH-SY5Y **(c)** or GMK **(d)** cell growth was analysed in the presence of 5μM ApoE isoforms. The data were normalized to the average absorbance values of the dissolvent group.

Fig. S2

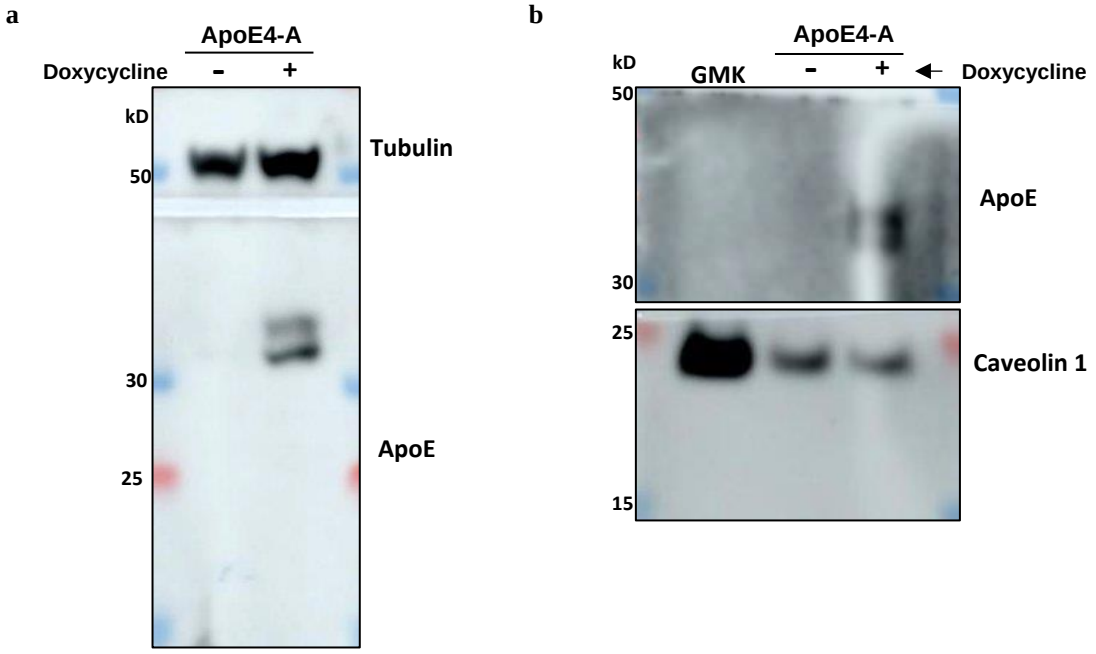

Fig. S2 Plasma membrane association of ApoE 4 in an ApoE 4 inducible cell line. (a) Induction of ApoE 4 by doxycycline. ApoE 4 inducible cells were prepared in large culture for membrane extraction. The expression of ApoE 4 was induced by adding doxycycline (1µg/mL) overnight (about 16h), before the cells were harvested for membrane extraction. Aliquots of both mock treated and induced cells were collected and analysed by western blot for ApoE expression. Tubulin was probed as a loading control. **(b)** Plasma membrane association of ApoE 4. The presence of ApoE 4 and caveolin 1 were verified by western blot in the extracted and purified plasma membrane samples.

Supplement materials and methods.

Cell proliferation test

Cell proliferation was evaluated by the WST-1 based colorimetric assay according to the manufacturer's instructions (Roche, 5015944001). In brief, cells were seeded in 96-well plates and cultured overnight. On the second day, medium was changed to 50 µL of new medium containing the designated ApoE and the cells were further cultured for 24h. 4h prior to analysis, WST-1 reagent was added (5µL per well), followed by the measurement of absorbance at 440nm by an ELISA reader. The corresponding culture medium was included as a control and this readout was subtracted from the experimental groups.

Acknowledgements: The authors would like to thank Tomas Bergström (Gothenburg university), Sigvard Olofsson (Gothenburg university), Jan Olsson (Umeå University) and Fredrik Elgh (Umeå University) for providing advice during the project development. Magnus Evander, Niklas Arnberg, and Anna Överby (Umeå University) are acknowledged for providing cells and plasmids. We also thank the Biochemical Imaging Center at Umeå University and the National Microscopy Infrastructure, NMI (VR-RFI 2019-00217) for providing assistance in microscopy. This project has been funded by the the Kempe foundation, the Knut and Alice Wallenberg foundation, Åhlensfonden, Alzheimerfonden, Norrländska hjärtfonden, Söderbergs stiftelse (M55/22), and the Swedish research council (2017-04029; 2020-06242).

Competing interests

The authors declare that they have no competing interests.

References

Abidine, Y., Liu, L., Wallén, O., Trybala, E., Olofsson, S., Bergström, T., & Bally, M. (2022). Cellular Chondroitin Sulfate and the Mucin-like Domain of Viral Glycoprotein C Promote Diffusion of Herpes Simplex Virus 1 While Heparan Sulfate Restricts Mobility. *Viruses*, *14*(8), 1836. https://doi.org/10.3390/v14081836

Ahmad, I., & Wilson, D. W. (2020). Hsv-1 cytoplasmic envelopment and egress. *International Journal of Molecular Sciences*, *21*(17), 1–34. https://doi.org/10.3390/ijms21175969

Altgärde, N., Eriksson, C., Peerboom, N., Phan-Xuan, T., Moeller, S., Schnabelrauch, M., Svedhem, S., Trybala, E., Bergström, T., & Bally, M. (2015). Mucin-like region of herpes simplex virus type 1 attachment protein glycoprotein C (gC) modulates the virus-glycosaminoglycan interaction. *Journal of Biological Chemistry*, *290*(35), 21473–21485. https://doi.org/10.1074/jbc.M115.637363

Ball, M. J. (1982). "Limbic predilection in Alzheimer dementia: is reactivated herpesvirus involved?". *The Canadian Journal of Neurological Sciences. Le Journal Canadien Des Sciences Neurologiques*, *9*(3), 303–306. https://doi.org/10.1017/s0317167100044115

Banfield, B. W., Leduc, Y., Esford, L., Visalli, R. J., Brandt, C. R., & Tufaro, F. (1995). Evidence for an Interaction of Herpes Simplex Virus with Chondroitin Sulfate Proteoglycans during Infection. *Virology*, *208*(2), 531–539. https://doi.org/10.1006/viro.1995.1184

Bankwitz, D., Doepke, M., Hueging, K., Weller, R., Bruening, J., Behrendt, P., Lee, J. Y., Vondran, F. W. R., Manns, M. P., Bartenschlager, R., & Pietschmann, T. (2017). Maturation of secreted HCV particles by incorporation of secreted ApoE protects from antibodies by enhancing infectivity. *J Hepatol*, *67*(3), 480–489. https://doi.org/10.1016/j.jhep.2017.04.010

Benga, W. J., Krieger, S. E., Dimitrova, M., Zeisel, M. B., Parnot, M., Lupberger, J., Hildt, E., Luo, G., McLauchlan, J., Baumert, T. F., & Schuster, C. (2010). Apolipoprotein E interacts with hepatitis C virus nonstructural protein 5A and determines assembly of infectious particles. *Hepatology*, *51*(1), 43–53. https://doi.org/10.1002/hep.23278

Bhattacharjee, P S, Neumann, D. M., Foster, T. P., Bouhanik, S., Clement, C., Vinay, D., Thompson, H. W., & Hill, J. M. (2008). Effect of human apolipoprotein E genotype on the pathogenesis of experimental ocular HSV-1. *Exp Eye Res*, *87*(2), 122–130. https://doi.org/10.1016/j.exer.2008.05.007

Bhattacharjee, P S, Neumann, D. M., Stark, D., Thompson, H. W., & Hill, J. M. (2006). Apolipoprotein E modulates establishment of HSV-1 latency and survival in a mouse ocular model. *Curr Eye Res*, *31*(9), 703–708. https://doi.org/10.1080/02713680600864600

Bhattacharjee, Partha S., Neumann, D. M., Foster, T. P., Clement, C., Singh, G., Thompson, H. W., Kaufman, H. E., & Hill, J. M. (2008). Effective treatment of ocular HSK with a human apolipoprotein E mimetic peptide in a mouse eye model. *Investigative Ophthalmology and Visual Science*, *49*(10), 4263–4268. https://doi.org/10.1167/iovs.08-2077

Bhattacharjee, Partha S, Neumann, D. M., & Hill, J. M. (2009). A Human Apolipoprotein E Mimetic Peptide Effectively Inhibits HSV-1 TK-Positive and TK-Negative Acute Epithelial Keratitis in Rabbits. *Current Eye Research*, *34*(2), 99–102. https://doi.org/10.1080/02713680802647662

Bi, F. C., Yang, X. H., Cheng, X. Y., Deng, W. Bin, Guo, X. L., Yang, H., Wang, Y., Li, J., & Yao, Y. (2021). Optimization of cerebral organoids: a more qualified model for Alzheimer's disease research. *Translational Neurodegeneration*, *10*(1), 1–13. https://doi.org/10.1186/s40035-021-00252-3

Brown, J. C. (2017). Herpes simplex virus latency: The DNA repair-Centered pathway. *Advances in Virology*, *2017*. https://doi.org/10.1155/2017/7028194

Burgos, J. S., Ramirez, C., Sastre, I., Bullido, M. J., & Valdivieso, F. (2002). Involvement of Apolipoprotein E in the Hematogenous Route of Herpes Simplex Virus Type 1 to the Central Nervous System. *Journal of Virology*, *76*(23), 12394–12398. https://doi.org/10.1128/jvi.76.23.12394-12398.2002

Burgos, J. S., Ramirez, C., Sastre, I., & Valdivieso, F. (2006). Effect of Apolipoprotein E on the Cerebral Load of Latent Herpes Simplex Virus Type 1 DNA. *Journal of Virology*, *80*(11), 5383–5387. https://doi.org/10.1128/jvi.00006-06

Chang, K. S., Jiang, J., Cai, Z., & Luo, G. (2007). Human apolipoprotein e is required for infectivity and production of hepatitis C virus in cell culture. *J Virol*, *81*(24), 13783–13793. https://doi.org/10.1128/JVI.01091-07

Cun, W., Jiang, J., & Luo, G. (2010). The C-terminal alpha-helix domain of apolipoprotein E is required for interaction with nonstructural protein 5A and assembly of hepatitis C virus. *J Virol*, *84*(21), 11532–11541. https://doi.org/10.1128/JVI.01021-10

Delguste, M., Peerboom, N., Le Brun, G., Trybala, E., Olofsson, S., Bergström, T., Alsteens, D., & Bally, M. (2019). Regulatory Mechanisms of the Mucin-Like Region on Herpes Simplex Virus during Cellular Attachment. *ACS Chemical Biology*, *14*(3), 534–542. https://doi.org/10.1021/acschembio.9b00064

Desai, P. J., Schaffer, P. A., & Minson, A. C. (1988). Excretion of non-infectious virus particles lacking glycoprotein H by a temperature-sensitive mutant of herpes simplex virus type 1: Evidence that gH is essential for virion infectivity. *Journal of General Virology*, *69*(6), 1147–

1156. https://doi.org/10.1099/0022-1317-69-6-1147

Dobson, C. B., Sales, S. D., Hoggard, P., Wozniak, M. A., & Crutcher, K. A. (2006). The receptor-binding region of human apolipoprotein E has direct anti-infective activity. *Journal of Infectious Diseases*, *193*(3), 442–450. https://doi.org/10.1086/499280

Dong, L. M., Parkin, S., Trakhanov, S. D., Rupp, B., Simmons, T., Arnold, K. S., Newhouse, Y. M., Innerarity, T. L., & Weisgraber, K. H. (1996). Novel mechanism for defective receptor binding of apolipoprotein E2 in type III hyperlipoproteinemia. *Nature Structural Biology*, *3*(8), 718–722. https://doi.org/10.1038/nsb0896-718

Dong, L. M., & Weisgraber, K. H. (1996). Human apolipoprotein E4 domain interaction. Arginine 61 and glutamic acid 255 interact to direct the preference for very low density lipoproteins. *The Journal of Biological Chemistry*, *271*(32), 19053–19057. https://doi.org/10.1074/jbc.271.32.19053

Elshourbagy, N. A., Boguski, M. S., Liao, W. S., Jefferson, L. S., Gordon, J. I., & Taylor, J. M. (1985). Expression of rat apolipoprotein A-IV and A-I genes: mRNA induction during development and in response to glucocorticoids and insulin. *Proceedings of the National Academy of Sciences of the United States of America*, *82*(23), 8242–8246. https://doi.org/10.1073/pnas.82.23.8242

Filén, F., Strand, A., Allard, A., Blomberg, J., & Herrmann, B. (2004). Duplex real-time polymerase chain reaction assay for detection and quantification of herpes simplex virus type 1 and herpes simplex virus type 2 in genital and cutaneous lesions. *Sexually Transmitted Diseases*, *31*(6), 331–336. https://doi.org/10.1097/00007435-200406000-00002

Futamura, M., Dhanasekaran, P., Handa, T., Phillips, M. C., Lund-Katz, S., & Saito, H. (2005). Two-step mechanism of binding of apolipoprotein E to heparin: Implications for the kinetics of apolipoprotein E-heparan sulfate proteoglycan complex formation on cell surfaces. *Journal of Biological Chemistry*, *280*(7), 5414–5422. https://doi.org/10.1074/jbc.M411719200

Gastaminza, P., Dryden, K. A., Boyd, B., Wood, M. R., Law, M., Yeager, M., & Chisari, F. V. (2010). Ultrastructural and Biophysical Characterization of Hepatitis C Virus Particles Produced in Cell Culture. *Journal of Virology*, *84*(21), 10999–11009. https://doi.org/10.1128/jvi.00526-10

Griffiths, G., Pfeiffer, S., Simons, K., & Matlin, K. (1985). Exit of newly synthesized membrane proteins from the trans cisterna of the golgi complex to the plasma membrane. *Journal of Cell Biology*, *101*(3), 949–964. https://doi.org/10.1083/jcb.101.3.949

Hadigal, S., Koganti, R., Yadavalli, T., Agelidis, A., Suryawanshi, R., & Shukla, D. (2020). Heparanase-Regulated Syndecan-1 Shedding Facilitates Herpes Simplex Virus 1 Egress. *Journal*

of Virology, *94*(6). https://doi.org/10.1128/jvi.01672-19

Hadigal, S. R., Agelidis, A. M., Karasneh, G. A., Antoine, T. E., Yakoub, A. M., Ramani, V. C., Djalilian, A. R., Sanderson, R. D., & Shukla, D. (2015). Heparanase is a host enzyme required for herpes simplex virus-1 release from cells. *Nature Communications*, *6*, 6985. https://doi.org/10.1038/ncomms7985

Herold, B. C., WuDunn, D., Soltys, N., & Spear, P. G. (1991). Glycoprotein C of herpes simplex virus type 1 plays a principal role in the adsorption of virus to cells and in infectivity. *Journal of Virology*, *65*(3), 1090–1098. https://doi.org/10.1128/jvi.65.3.1090-1098.1991

Hogue, I. B., Bosse, J. B., Hu, J.-R., Thiberge, S. Y., & Enquist, L. W. (2014). Cellular mechanisms of alpha herpesvirus egress: live cell fluorescence microscopy of pseudorabies virus exocytosis. *PLoS Pathogens*, *10*(12), e1004535. https://doi.org/10.1371/journal.ppat.1004535

Hopkins, J., Yadavalli, T., Agelidis, A. M., & Shukla, D. (2018a). Host Enzymes Heparanase and Cathepsin L Promote Herpes Simplex Virus 2 Release from Cells. *Journal of Virology*, *92*(23). https://doi.org/10.1128/jvi.01179-18

Hopkins, J., Yadavalli, T., Agelidis, A. M., & Shukla, D. (2018b). Host Enzymes Heparanase and Cathepsin L Promote Herpes Simplex Virus 2 Release from Cells. *Journal of Virology*, *92*(23). https://doi.org/10.1128/JVI.01179-18

Huemer, H. P., Menzel, H. J., Potratz, D., Brake, B., Falke, D., Utermann, G., & Dierich, M. P. (1988). Herpes simplex virus binds to human serum lipoprotein. *Intervirology*, *29*(2), 68–76. https://doi.org/10.1159/000150031

Itzhaki, R. F., Dobson, C. B., Lin, W. R., & Wozniak, M. A. (2001). Association of HSV1 and apolipoprotein E-ε4 in Alzheimer's disease. *Journal of NeuroVirology*, *7*(6), 570–571. https://doi.org/10.1080/135502801753248169

Itzhaki, Ruth F., Lin, W. R., Shang, D., Wilcock, G. K., Faragher, B., & Jamieson, G. A. (1997). Herpes simplex virus type 1 in brain and risk of Alzheimer's disease. *Lancet*, *349*(9047), 241–244. https://doi.org/10.1016/S0140-6736(96)10149-5

Jiang, J., & Luo, G. (2009). Apolipoprotein E but not B is required for the formation of infectious hepatitis C virus particles. *J Virol*, *83*(24), 12680–12691. https://doi.org/10.1128/JVI.01476-09

Jiang, J., Wu, X., Tang, H., & Luo, G. (2013). Apolipoprotein E mediates attachment of clinical hepatitis C virus to hepatocytes by binding to cell surface heparan sulfate proteoglycan receptors. *PLoS One*, *8*(7), e67982. https://doi.org/10.1371/journal.pone.0067982

Kim, J., Basak, J. M., & Holtzman, D. M. (2009). The Role of Apolipoprotein E in Alzheimer's

Disease. *Neuron*, *63*(3), 287–303. https://doi.org/10.1016/j.neuron.2009.06.026

Kuhlmann, I., Minihane, A. M., Huebbe, P., Nebel, A., & Rimbach, G. (2010). Apolipoprotein e genotype and hepatitis C, HIV and herpes simplex disease risk: A literature review. *Lipids in Health and Disease*, *9*, 1–14. https://doi.org/10.1186/1476-511X-9-8

Ladu, M. J., Stine, W. B., Narita, M., Getz, G. S., Reardon, C. A., & Bu, G. (2006). Self-assembly of HEK cell-secreted ApoE particles resembles ApoE enrichment of lipoproteins as a ligand for the LDL receptor-related protein. *Biochemistry*, *45*(2), 381–390. https://doi.org/10.1021/bi051765s

Lee, J. Y., Acosta, E. G., Stoeck, I. K., Long, G., Hiet, M. S., Mueller, B., Fackler, O. T., Kallis, S., & Bartenschlager, R. (2014). Apolipoprotein E likely contributes to a maturation step of infectious hepatitis C virus particles and interacts with viral envelope glycoproteins. *J Virol*, *88*(21), 12422–12437. https://doi.org/10.1128/JVI.01660-14

Li, Y., & Luo, G. (2021). Human low-density lipoprotein receptor plays an important role in hepatitis B virus infection. *PLoS Pathogens*, *17*(7), 1–21. https://doi.org/10.1371/journal.ppat.1009722

Libeu, C. P., Lund-Katz, S., Phillips, M. C., Wehrli, S., Hernáiz, M. J., Capila, I., Linhardt, R. J., Raffaï, R. L., Newhouse, Y. M., Zhou, F., & Weisgraber, K. H. (2001). New Insights into the Heparan Sulfate Proteoglycan-binding Activity of Apolipoprotein E. *Journal of Biological Chemistry*, *276*(42), 39138–39144. https://doi.org/10.1074/jbc.M104746200

LIN, W.-R., SHANG, D., WILCOCK, G. K., & ITZHAKI, R. F. (1995). Alzheimer's disease, herpes simplex virus type 1, cold sores and apolipoprotein E4. *Biochemical Society Transactions*, *23*(4), 594S-594S. https://doi.org/10.1042/bst023594s

Lin, W. R., Shang, D., & Itzhaki, R. F. (1996). Neurotropic viruses and Alzheimer disease: Interaction of herpes simplex type I virus and apolipoprotein E in the etiology of the disease. *Molecular and Chemical Neuropathology*, *28*(1–3), 135–141. https://doi.org/10.1007/BF02815215

Linard, M., Letenneur, L., Garrigue, I., Doize, A., Dartigues, J. F., & Helmer, C. (2020). Interaction between APOE4 and herpes simplex virus type 1 in Alzheimer's disease. *Alzheimers Dement*, *16*(1), 200–208. https://doi.org/10.1002/alz.12008

Lopatko Lindman, K, Weidung, B., Olsson, J., Josefsson, M., Kok, E., Johansson, A., Eriksson, S., Hallmans, G., Elgh, F., & Lovheim, H. (2019). A genetic signature including apolipoprotein Eepsilon4 potentiates the risk of herpes simplex-associated Alzheimer's disease. *Alzheimers Dement (N Y)*, *5*, 697–704. https://doi.org/10.1016/j.trci.2019.09.014

Lopatko Lindman, Karin, Lockman-Lundgren, J., Weidung, B., Olsson, J., Elgh, F., & Lövheim, H. (2022). Long-term time trends in reactivated herpes simplex infections and treatment in

Sweden. *BMC Infectious Diseases*, *22*(1), 547. https://doi.org/10.1186/s12879-022-07525-w

Lövheim, H., Norman, T., Weidung, B., Olsson, J., Josefsson, M., Adolfsson, R., Nyberg, L., & Elgh, F. (2019). Herpes Simplex Virus, APOE ϵ4, and Cognitive Decline in Old Age: Results from the Betula Cohort Study. *Journal of Alzheimer's Disease*, *67*(1), 211–220. https://doi.org/10.3233/JAD-171162

Mahley, R. W., & Rall Jr., S. C. (2000). Apolipoprotein E: far more than a lipid transport protein. *Annu Rev Genomics Hum Genet*, *1*, 507–537. https://doi.org/10.1146/annurev.genom.1.1.507

Marconi, P., & Manservigi, R. (2014). Herpes simplex virus growth, preparation, and assay. *Methods in Molecular Biology (Clifton, N.J.)*, *1144*, 19–29. https://doi.org/10.1007/978-1-4939-0428-0_2

Martens, Y. A., Xu, S., Tait, R., Li, G., Zhao, X. C., Lu, W., Liu, C.-C., Kanekiyo, T., Bu, G., & Zhao, J. (2021). Generation and validation of APOE knockout human iPSC-derived cerebral organoids. *STAR Protocols*, *2*(2), 100571. https://doi.org/10.1016/j.xpro.2021.100571

Miller, R. M., & Federoff, H. J. (2008). Isoform-specific effects of ApoE on HSV immediate early gene expression and establishment of latency. *Neurobiol Aging*, *29*(1), 71–77. https://doi.org/10.1016/j.neurobiolaging.2006.09.006

Mingo, R. M., Han, J., Newcomb, W. W., & Brown, J. C. (2012). Replication of Herpes Simplex Virus: Egress of Progeny Virus at Specialized Cell Membrane Sites. *Journal of Virology*, *86*(13), 7084–7097. https://doi.org/10.1128/jvi.00463-12

Myklebost, O., & Rogne, S. (1988). A physical map of the apolipoprotein gene cluster on human chromosome 19. *Human Genetics*, *78*(3), 244–247. https://doi.org/10.1007/BF00291670

Nicola, A. V, & Straus, S. E. (2004). Cellular and viral requirements for rapid endocytic entry of herpes simplex virus. *J Virol*, *78*(14), 7508–7517. https://doi.org/10.1128/JVI.78.14.7508-7517.2004

O'Keeffe, R., Johnston, M. D., & Slater, N. K. H. (1998). The primary production of an infectious recombinant herpes simplex virus vaccine. *Biotechnology and Bioengineering*, *57*(3), 262–271. https://doi.org/10.1002/(SICI)1097-0290(19980205)57:3<262::AID-BIT2>3.0.CO;2-F

Pace, H., Simonsson Nyström, L., Gunnarsson, A., Eck, E., Monson, C., Geschwindner, S., Snijder, A., & Höök, F. (2015). Preserved transmembrane protein mobility in polymer-supported lipid bilayers derived from cell membranes. *Analytical Chemistry*, *87*(18), 9194–9203. https://doi.org/10.1021/acs.analchem.5b01449

Pandey, J. P., Olsson, J., Weidung, B., Kothera, R. T., Johansson, A., Eriksson, S., Hallmans, G., Elgh, F., & Lövheim, H. (2020). An Ig γ Marker Genotype Is a Strong Risk Factor for

Alzheimer Disease, Independent of Apolipoprotein E ε4 Genotype. *Journal of Immunology (Baltimore, Md. : 1950)*, *205*(5), 1318–1322. https://doi.org/10.4049/jimmunol.2000351

Park, D., Lalli, J., Sedlackova-Slavikova, L., & Rice, S. A. (2015). Functional Comparison of Herpes Simplex Virus 1 (HSV-1) and HSV-2 ICP27 Homologs Reveals a Role for ICP27 in Virion Release. *Journal of Virology*, *89*(5), 2892–2905. https://doi.org/10.1128/jvi.02994-14

Peerboom, N., Block, S., Altgärde, N., Wahlsten, O., Möller, S., Schnabelrauch, M., Trybala, E., Bergström, T., & Bally, M. (2017). Binding Kinetics and Lateral Mobility of HSV-1 on End-Grafted Sulfated Glycosaminoglycans. *Biophysical Journal*, *113*(6), 1223–1234. https://doi.org/10.1016/j.bpj.2017.06.028

Peerboom, N., Schmidt, E., Trybala, E., Block, S., Bergström, T., Pace, H. P., & Bally, M. (2018). Cell Membrane Derived Platform To Study Virus Binding Kinetics and Diffusion with Single Particle Sensitivity. *ACS Infectious Diseases*, *4*(6), 944–953. https://doi.org/10.1021/acsinfecdis.7b00270

Qiao, L., & Luo, G. G. (2019). Human apolipoprotein E promotes hepatitis B virus infection and production. *PLoS Pathog*, *15*(8), e1007874. https://doi.org/10.1371/journal.ppat.1007874

Saito, H., Dhanasekaran, P., Nguyen, D., Baldwin, F., Weisgraber, K. H., Wehrli, S., Phillips, M. C., & Lund-Katz, S. (2003). Characterization of the heparin binding sites in human apolipoprotein E. *Journal of Biological Chemistry*, *278*(17), 14782–14787. https://doi.org/10.1074/jbc.M213207200

Schindelin, J., Arganda-Carreras, I., Frise, E., Kaynig, V., Longair, M., Pietzsch, T., Preibisch, S., Rueden, C., Saalfeld, S., Schmid, B., Tinevez, J. Y., White, D. J., Hartenstein, V., Eliceiri, K., Tomancak, P., & Cardona, A. (2012). Fiji: An open-source platform for biological-image analysis. *Nature Methods*, *9*(7), 676–682. https://doi.org/10.1038/nmeth.2019

Shieh, M. T., WuDunn, D., Montgomery, R. I., Esko, J. D., & Spear, P. G. (1992). Cell surface receptors for herpes simplex virus are heparan sulfate proteoglycans. *J Cell Biol*, *116*(5), 1273–1281. https://doi.org/10.1083/jcb.116.5.1273

Siddiqui, R., Suzu, S., Ueno, M., Nasser, H., Koba, R., Bhuyan, F., Noyori, O., Hamidi, S., Sheng, G., Yasuda-Inoue, M., Hishiki, T., Sukegawa, S., Miyagi, E., Strebel, K., Matsushita, S., Shimotohno, K., & Ariumi, Y. (2018). Apolipoprotein E is an HIV-1-inducible inhibitor of viral production and infectivity in macrophages. *PLoS Pathogens*, *14*(11), e1007372. https://doi.org/10.1371/journal.ppat.1007372

Steel, A. J., & Eslick, G. D. (2015). Herpes viruses increase the risk of Alzheimer's disease: A meta-analysis. *Journal of Alzheimer's Disease*, *47*(2), 351–364. https://doi.org/10.3233/JAD-140822

Strandberg, T. E., Pitkala, K., Eerola, J., Tilvis, R., & Tienari, P. J. (2005). Interaction of herpesviridae, APOE gene, and education in cognitive impairment. *Neurobiology of Aging*, *26*(7), 1001–1004. https://doi.org/10.1016/j.neurobiolaging.2004.09.008

Thorsteinsson, K., Olsén, E., Schmidt, E., Pace, H., & Bally, M. (2020). FRET-Based Assay for the Quantification of Extracellular Vesicles and Other Vesicles of Complex Composition. *Analytical Chemistry*, *92*(23), 15336–15343. https://doi.org/10.1021/acs.analchem.0c02271

Trybala, E, Liljeqvist, J. A., Svennerholm, B., & Bergström, T. (2000). Herpes simplex virus types 1 and 2 differ in their interaction with heparan sulfate. *J Virol*, *74*(19), 9106–9114. https://doi.org/10.1128/jvi.74.19.9106-9114.2000

Trybala, Edward, Peerboom, N., Adamiak, B., Krzyzowska, M., Liljeqvist, J.-Å., Bally, M., & Bergström, T. (2021). Herpes Simplex Virus Type 2 Mucin-Like Glycoprotein mgG Promotes Virus Release from the Surface of Infected Cells. *Viruses*, *13*(5), 887. https://doi.org/10.3390/v13050887

Tudorache, I. F., Trusca, V. G., & Gafencu, A. V. (2017). Apolipoprotein E - A Multifunctional Protein with Implications in Various Pathologies as a Result of Its Structural Features. *Comput Struct Biotechnol J*, *15*, 359–365. https://doi.org/10.1016/j.csbj.2017.05.003

Wainberg, M., Luquez, T., Koelle, D. M., Readhead, B., Johnston, C., Darvas, M., & Funk, C. C. (2021). The viral hypothesis: how herpesviruses may contribute to Alzheimer's disease. *Molecular Psychiatry*, *26*(10), 5476–5480. https://doi.org/10.1038/s41380-021-01138-6

Xu, Y., Martinez, P., Séron, K., Luo, G., Allain, F., Dubuisson, J., & Belouzard, S. (2015). Characterization of Hepatitis C Virus Interaction with Heparan Sulfate Proteoglycans. *Journal of Virology*, *89*(7), 3846–3858. https://doi.org/10.1128/jvi.03647-14

Yamauchi, Y., Deguchi, N., Takagi, C., Tanaka, M., Dhanasekaran, P., Nakano, M., Handa, T., Phillips, M. C., Lund-Katz, S., & Saito, H. (2008). Role of the N- and C-terminal domains in binding of apolipoprotein E isoforms to heparan sulfate and dermatan sulfate: A surface plasmon resonance study. *Biochemistry*, *47*(25), 6702–6710. https://doi.org/10.1021/bi8003999

Ye, S. Q., Reardon, C. A., & Getz, G. S. (1993). Inhibition of apolipoprotein E degradation in a post-Golgi compartment by a cysteine protease inhibitor. *Journal of Biological Chemistry*, *268*(12), 8497–8502. https://doi.org/10.1016/s0021-9258(18)52902-1

Yue, L., & Mazzone, T. (2011). Endogenous adipocyte apolipoprotein E is colocalized with caveolin at the adipocyte plasma membrane. *Journal of Lipid Research*, *52*(3), 489–498. https://doi.org/10.1194/jlr.M011809

1145